Journal of Geosciences, 62 (2017), 37–57 DOI: 10.3190/jgeosci.235

Original paper

Lillianite homologues from Kutná Hora ore district, Czech Republic: a case of large-scale Sb for Bi substitution

Richard PAŽOUT

University of Chemistry and Technology Prague, Technická 5, 166 28 Prague 6, Czech Republic; richard.pazout@vscht.cz

Numerous complex Ag–Pb–Bi–Sb sulphosalt minerals belonging to the lillianite homologous series previously unknown in Czech Republic, including a new mineral species, have been identified in samples from hydrothermal vein mineralization of the Kutná Hora Ag–Pb–Zn ore district, central Bohemia, Czech Republic. Identified lillianite homologues include both Bi members (minerals of the lillianite branch) and Sb members (andorite branch) and show an extensive Sb for Bi substitution. Nine distinct compositional groups were identified among Bi members, corresponding to: N = 4 (gustavite, terrywallaceite, staročeskéite – recently approved IMA No. 2016-101), N = 5.5 (vikingite), N = 6 (treasurite), N = 7 (eskimoite and (Ag, Bi)-rich heyrovskýite), N = 8 (erzwiesite) and schirmerite (Type 2). Single-crystal XRD measurement of Bi members with N = 4 revealed a new mineral, staročeskéite. Unlike gustavite and terrywallaceite, which are monoclinic, staročeskéite is orthorhombic with $a = 4.2539(8)$, $b = 13.3094(8)$, $c = 19.625(1)$ Å, and the ideal formula is $Ag_{0.70}Pb_{1.60}(Bi_{1.35}Sb_{1.35})_{\Sigma 2.70}S_6$, corresponding to $N_{chem} = 4$, Bi/(Bi + Sb) = 0.50 and substitution percentage L% = 70. Among Sb members, minerals with N = 4 (andorite series) and N = 5.0–5.5 were found. Relations between substitution percentage, chemical N and Sb content have been observed. The description of the new occurrence of Bi sulphosalts, including Sb-rich varieties and a continuous transition from Bi-dominant to Sb-dominant phases with N = 4 provides new information on compositional limits in natural sulphosalts. Comparable range of the $Bi^{3+} \leftrightarrow Sb^{3+}$substitution in lillianite homologues with N = 4 has not been observed before.

Keywords: bismuth lillianite homologues, andorite series, chemistry, powder and single-crystal X-ray diffraction, Kutná Hora, Czech Republic

Received: 23 March, 2016; accepted: 7 April, 2017; handling editor: R. Skála

The online version of this article (doi: 10.3190/jgeosci.235) contains supplementary electronic material.

1. Introduction

Lillianite homologous series is derived from the structure of lillianite, $Pb_3Bi_2S_6$, and it is the oldest and most prolific homologous series of sulphosalts, a typical example of an accretional series. Members of this series are complex Pb–Bi–Sb–Ag sulphides with structures consisting of alternating layers of PbS archetype cut parallel to $(311)_{PbS}$. The octahedra of adjacent, mirror-related layers are replaced by bi-capped trigonal coordination prisms of PbS_{6+2} with the Pb atoms positioned on the mirror planes (Otto and Strunz 1968). Detailed description of the series was provided by Makovicky and Topa (2014).

Members of this series differ in the thickness of the PbS-like layers and they are characterized by the order number (N) of the homologue corresponding to the number of octahedra diagonally across the slab thickness; prisms are excluded. This value can be determined either from the crystal structure (N_{cryst}) or from the chemical analysis (N_{chem}), where $N_{chem} = N_{aver} = (N1_{cryst} + N2_{cryst})/2$ for two adjacent slabs. For example vikingite has $N1_{cryst} = 4$, $N2_{cryst} = 7$, $N_{chem} = 5.5$. The number of octahedra in two adjacent (neighbouring) chains separated by Pb atoms in trigonal coordination can be the same (known combinations for minerals are 4–4, 7–7, 8–8 or 11–11) or different (known combinations are 4–7, 4–8 and 5–9). Minerals with N1 = N2 are orthorhombic (with symmetry sometimes reduced to monoclinic because of cation ordering), and minerals with N1 ≠ N2 monoclinic (or triclinic because of cation ordering).

The values of N_{chem}, the substitution percentage (L%) of the $Ag^+ + Bi^{3+} \leftrightarrow 2\ Pb^{2+}$ substitution and substitution coefficient x can be calculated from measured Pb : Bi : Ag atomic ratios according to the formulae derived by Makovicky and Karup-Møller (1977a). Each lillianite homologue can be described as $^{N1,N2}L$ (L stands for a lillianite homologue) where N1 and N2 are the numbers of octahedra for two adjacent sets of layers. General chemical formula is $Pb_{N-1-2x}Bi_{2+x}Ag_xS_{N+2}$ (Z = 4) where $N = N_{chem} = (N1 + N2)/2$ and x is the substitution coefficient for the $Ag^+ + Bi^{3+} \leftrightarrow 2\ Pb^{2+}$ substitution. Two major substitutions play a decisive role in the crystal chemistry of lillianite homologues:

(1) $Ag^+ + Bi^{3+} \leftrightarrow 2\ Pb^{2+}$ for Bi lillianite homologues or $Ag^+ + Sb^{3+} \leftrightarrow 2\ Pb^{2+}$ for Sb ones. This substitution is expressed as a subscript past the phase symbol. For instance gustavite with 85 % of the above substitution is referred

to as Gus_{85}. In the lillianite–gustavite solid solution with N = 4, the two end members are: lillianite – $Pb_3Bi_2S_6$, 0% of the $Ag^+ + Bi^{3+} \leftrightarrow 2\ Pb^{2+}$ substitution, $^4L_0$, and gustavite – $AgPbBi_3S_6$, 100% substitution, $^4L_{100}$.

(2) $Bi^{3+} \leftrightarrow Sb^{3+}$ substitution is proposed in this paper to be expressed as a superscript past the phase symbol. The Bi–Sb substitution is expressed in terms of Bi/(Bi + Sb) atomic ratio multiplied by 100, an ideal gustavite with no Sb being $^4Gus^{100}_{100}$ and an ideal andorite VI with no Bi being $^4And^{0}_{100}$. Thus, a full description of any lillianite homologue can be expressed as $^NL^{Bi-Sb}_{L\%}$.

Natural bismuthian lillianite homologues are: lillianite $Pb_3Bi_2S_6$ (^{4,4}L), xilingolite $Pb_3Bi_2S_6$ (^{4,4}L), gustavite $PbAgBi_3S_6$ (^{4,4}L), terrywallaceite $AgPb(Sb,Bi)(Bi,Sb)_2S_6$ (^{4,4}L), schirmerite (disordered), vikingite $Pb_8Ag_5Bi_{13}S_{30}$ (^{4,7}L), treasurite $Pb_6Ag_7Bi_{15}S_{32}$ (^{4,8}L), eskimoite $Pb_{10}Ag_7Bi_{15}S_{36}$ (^{5,9}L), heyrovskýite $Pb_6Bi_2S_9$ (^{7,7}L), aschalmamite $Pb_6Bi_2S_9$ (^{7,7}L), erzwiesite $Pb_3Ag_2Bi_4S_{10}$ (^{8,8}L) and ourayite $Pb_4Ag_3Bi_5S_{13}$ (^{11,11}L) (Makovicky and Topa 2014).

Natural antimonian lillianite homologues are known only for N = 4 (^{4,4}L) and include minerals differing by the $Ag^+ + Sb^{3+} \leftrightarrow 2\ Pb^{2+}$ substitution percentage L% and by unit-cell parameter (Moëlo et al. 1989; Makovicky and Topa 2014). Andorite VI is defined as a phase with substitution percentage L% = 100, formula $AgPbSb_3S_6$ (And_{100}) and the *c* parameter six times that of the subcell *c* = 6c' (c' ≈ 4 Å, subcell parameter). Andorite IV is defined as a phase with substitution percentage L% = 93.75, $Ag_{15}Pb_{18}Sb_{47}S_{96}$ ($And_{93.75}$) and *c* = 4c' (c' ≈ 4 Å). Ramdohrite $(Cd,Mn,Fe)Ag_{5.5}Pb_{12}Sb_{21.5}S_{48}$ is $And_{68.75}$ with *c* = 8.73 Å and fizelyite, $Ag_5Pb_{14}Sb_{21}S_{48}$, is $And_{62.5}$ with *c* = 8.68 Å. All four minerals have *a* ≈ 13 Å and *b* ≈ 19 Å. Mn-bearing uchucchacuaite $Pb_3MnAgSb_5S_{12}$ is And_{50}. No natural members with L% < 50 % are known. The oversubstituted end of the series includes five recently described mineral species: arsenquatrandorite $Pb_{12.8}Ag_{17.6}Sb_{38.08}As_{11,52}S_{96}$ (And_{110}), roshchinite $Pb_{10}Ag_{19}Sb_{51}S_{96}$ (And_{115}), oscarkempffite $Pb_4Ag_{10}Sb_{17}Bi_9S_{48}$ (And_{124}), clino-oscarkempffite $Pb_6Ag_{15}Sb_{21}Bi_{18}S_{72}$ (And_{125}) and jasrouxite $Pb_4Ag_{16}Sb_{24}As_{16}S_{72}$ ($And_{136.5}$). The oversubstitution takes place by replacing of Pb atom in trigonal prismatic coordination (Makovicky and Topa 2014).

A significantly increased extent of Sb for Bi substitution in lillianite homologues is rare in nature. Although many descriptions have indicated the presence of minor amounts of Sb, these seldom exceed Bi/(Bi + Sb) = 0.92. According to Cook (1997), only four occurrences of members of the lillianite–gustavite solid solution series containing significant Sb contents have been reported. In the Darwin vein deposit, California, the degree of Sb substitution in terms of Bi/(Bi + Sb) is between 0.84–0.88. From Rotgülden, Austria, the Sb-gustavite with up to 10.4 wt. % Sb (corresponding to Bi/(Bi + Sb) = 0.70) was reported in association with Sb minerals.

Although there are both Bi (lillianite branch) as well as Sb lillianite homologues (andorite branch), a mutual mixing of the two elements in one mineral was only limited until the recent discovery of terrywallaceite, oscarkempffite, clino-oscarkempffite and staročeskéite (newly approved IMA No. 2016-101). Most recently, a complete transition from gustavite with no or very little Sb through Sb-rich gustavite and terrywallaceite to staročeskéite with Bi/(Bi + Sb) = 0.50 further to andorite with Bi/(Bi + Sb) = 0.23 was found in the Kutná Hora ore district, central Bohemia, Czech Republic (this paper). A complete transition is observable even within one grain and appears as zoning of varying shades of grey with no distinguishable phase boundary in BSE images.

2. Geological setting

All studied samples come from the Staročeské pásmo Lode (Old Bohemian Lode) of the Kutná Hora Ag–Pb–Zn ore district, 60 km east of Prague, Czech Republic. Geological situation, mineralogy and geochemistry of the ore district were described by Holub et al. (1982), Malec and Pauliš (1997), Pauliš (1998) and Pažout et al. (2017). The samples were collected in the material from medieval mine dumps in 1999–2015, therefore no information is available on their in-situ position in individual vein structures. Only a small part of the studied samples comes from recent mining and geological survey activity in the 1960's.

The Staročeské pásmo Lode was mined from the discovery and opening of the ore district in the second half of the 13th century until the end of large-scale mining in the first half of 17th century. It is estimated that some 350 to 500 t of silver were extracted from this lode, far more than from any other lode of the ore district including the Ag-rich ones in the South (Pauliš 1998). The second peak of mining activity in the Kutná Hora ore district was made possible owing to the discovery of a new rich deposit, the Benátecká Vein of the Staročeské pásmo Lode, in the second half of the 16th century. The vein was not discovered by previous old miners because it does not crop out. Its Ag-rich pyrite vein with Fe–Cu–Sn–Zn–As–(Ag–Pb–Bi–Sb), up to two metres thick, produced estimated 100 t of silver in less than 40 years (Holub 2009). This vein was a subject of a small-scale mining carried out within geological survey in the 1960's which made it possible to study the mineralogical composition of these ores.

3. Analytical techniques

3.1. Chemical analyses

Some 145 polished sections (1500 point analyses), prepared from a representative number of ore specimens collected during field work in 1999–2015, were investigated microscopically and subsequently analysed by electron microprobe at the University of Salzburg. Quantitative chemical analysis was performed with a JEOL JXA-8600 electron microprobe (EPMA) in the wave-length dispersive mode (WDS), controlled by a LINK*eXL* system, operated at 25 kV, 35 nA, 20 s counting time for peaks and 7 s for background, and a beam diameter of 5 μm. The following standards and X-ray lines were used: $CuFeS_2$ (CuK_α, FeK_α), Ag (AgL_α), PbS (PbL_α), Bi_2S_3 (BiL_α, SK_α), Sb_2S_3 (SbL_α), CdTe (CdL_β, TeL_α), Bi_2Te_2S (BiL_α, TeL_α), Bi_2Se_3 (SeK_α). Raw data were corrected with an online ZAF-4 procedure. A second large set of polished sections with Bi-sulphosalts (560 points) was measured on CAMECA SX 100 WDS electron microprobe analyser at the National Museum, Prague in 2015. The analytical conditions were as follows: accelerating voltage of 25 kV, beam current of 20 nA, electron-beam diameter of 2 μm and standards: chalcopyrite (SK_α), Bi_2Se_3 (BiM_β), PbS (PbM_α), Ag (AgL_α), halite (ClK_α), Sb_2S_3 (SbL_α), CdTe (CdL_α), HgTe (HgM_α), pyrite (FeK_α), Cu (CuK_α), ZnS (ZnK_α), NiAs (AsL_α) and PbSe (SeL_β). Measured data were corrected using PAP software (Pouchou and Pichoir 1985).

Only point analyses with totals between 98 and 102 wt. % were considered and included (unless stated otherwise). All measured compositions are shown in Electronic Supplementary Material 1. Chemical analyses are grouped according to individual samples to show compositional changes within grains. The means of the analyses corresponding to an expected particular mineral species within each grain are ordered from the highest Bi/(Bi + Sb) ratio to the lowest. Phases with Bi/(Bi + Sb) > 0.75 are termed gustavite (Gus), and those with Bi/(Bi + Sb) = 0.50–0.75 terrywallaceite (Ter); both are calculated to 11 atoms per formula unit (*apfu*). Phases with Bi/(Bi + Sb) < 0.50 are arbitrarily labelled andorite (And) and calculated to 44 *apfu*, and those with Bi/(Bi + Sb) = 0.43–0.56 and substitution close to 70 % belong to the new mineral staročeskéite (Sta). The number after the phase symbol is the $Ag^+ + Bi^{3+} \leftrightarrow 2\ Pb^{2+}$ substitution percentage or $Ag^+ + Sb^{3+} \leftrightarrow 2\ Pb^{2+}$ substitution percentage in the case of andorite branch minerals, respectively.

3.2. Powder X-ray diffraction (P-XRD)

Powder X-ray diffraction data were collected on the Panalytical X'Pert PRO diffractometer (step-scanning 0.02°/30 s, radiation CuK_α, 40 kV, 30 mA, angular range 3.3–55° 2θ) equipped with a point detector and secondary graphite monochromator (University of Chemistry and Technology Prague). A very small amount of the sample was placed on the surface of a silicon sample holder. Quartz (if contained) in the analyzed sample was used as an internal standard to check the possible sample surface displacement. The obtained powder pattern was processed using the P-XRD software HighScore Plus (Degen et al. 2014) to find angular positions and intensities of reflections. The *hkl* indices were assigned according to Pažout et al. (2001) (PDF card 053–1159) in the case of gustavite, in other cases as indicated in tables of unit-cell parameters. The refinement of unit-cell parameters was carried out by least-squares method implemented in the program Firestar-2 (Fergusson et al. 1987), used extrapolation function: $\cos\theta \times \cot\theta + \cot^2\theta$.

A special attention was paid to the detection of gustavite diffraction lines corresponding to d_{060} and d_{004} to visually check the correctness of the refined *b* and *c* parameter while *β* was assumed to be 107.2°, a value most often quoted in previous studies (Harris and Chen 1975) and also most often refined from P-XRD data in this study, and to reflections corresponding to d_{150} (strongest line in the powder pattern of the gustavite) and $d_{140.}$ Only few gustavite powder patterns showed a distinctive (020) reflection corresponding to d_{020} ~ 9.8 Å, while the d_{060} reflection (*c*. 3.27 Å) was not detectable if quartz was present in the sample. Only exceptionally the pattern was identical to $^4Gus_{100}$ gustavite from Kutná Hora (Pažout et al. 2001). Frequently the patterns displayed a shift or a split of the strongest diffraction lines. The lines corresponding to d_{150}, d_{140} tended to display a shift reflecting chemical composition of the samples quite profoundly. The same applied to lines in the powder pattern of vikingite corresponding to d_{400} and $d_{0.0.12}$.

3.3. Single-crystal X-ray diffraction (S-XRD)

X-ray diffraction data were collected at ambient temperature on the single-crystal diffractometer Gemini (Oxford Diffraction) with CCD area detector Atlas using monochromatic MoK_α radiation (λK_α = 0.71073 Å) collimated by Mo Enhance collimator. Sample–detector distance was set to 100 mm. The determination of unit-cell parameters, integration of the CCD images and data reduction was done by program CrysAlis RED (Oxford Diffraction 2008). The same program was used for indexing of the crystal shape, its refinement and absorption correction. An additional refinement of crystal shape together with face angles was carried out by the program X-Shape (Stoe and Cie 1998). The structural model was found by the charge flipping method using the program Superflip (Palatinus and Chapuis 2007) and

refined and further processed by JANA2006 (Petříček et al. 2006).

4. Results – minerals of the lillianite homologous series and their chemical and structural properties

4.1. Lillianite homologues with Bi > Sb: lillianite branch

Minerals of the series form grains, lamellae and grain aggregates with maximum size of 30 by 20 mm and occasional crystals up to 2 mm with silver grey colour and strong metallic lustre. They are frequently intergrown with other lillianite homologues and galena, occasionally accompanied by izoklakeite, cosalite, aramayoite, matildite, native Bi, ikunolite, and Bi-rich Pb–Sb sulphosalts (jamesonite, boulangerite and owyheeite) (Pažout et al. 2017). They are indistinguishable in optical microscope as well as in BSE images. Back-scattered electron images, however, reflect the Sb for Bi substitution very well (vikingite is not distinguishable from cosalite or izoklakeite, but gustavite is brighter than terrywallaceite). Exsolution phenomena (observable within the used resolution) are rare and were seen only in several polished sections.

The bismuth sulphosalt assemblage originated from later stage, low-T fluids different from high-T stage of base sulphides of Fe, Zn, Cu, Sn and As; the two stages were separated by a tectonic event. Quite often, the Bi sulphosalts, native Bi and Ag,Pb-rich galena fill in fissures in older base sulphide vein filling (Pažout et al. 2017).

4.1.1. Lillianite homologues with N = 4

The gustavite–lillianite series of Bi lillianite homologues with N = 4 comprises three minerals with very similar characteristics. Gustavite and terrywallaceite were found in majority of analysed samples. Gustavite is the most frequent (*c*. 350 points), followed by terrywallaceite (330 points); staročeskéite was found in 17 samples (36 points).

Single-crystal diffraction experiments were carried out on fragments of members with N = 4 extracted from polished sections analyzed by microprobe. They showed that both fully substituted and oversubstituted gustavite and terrywallaceite display gustavite monoclinic unit cell; gustavite with L% = 84 and Bi/(Bi + Sb) = 0.85 still showed the same monoclinic unit cell, as did gustavite with L% = 71 and Bi/(Bi + Sb) = 0.91. However, a homogenous grain with N = 4, L% = 70 and Bi/(Bi + Sb) = 0.50 displayed the lillianite orthorhombic unit cell and the structure revealed one of its mix sites to have prevailing Sb occupancy. This mineral has orthorhombic symmetry, space group *Cmcm*, with a = 4.2539(8), b = 13.3094(8), c = 19.625(1) Å, V = 1111.1(2) Å^3, Z = 4 and was recently approved under the name of staročeskéite.

In powder patterns, the criterion for distinguishing between the monoclinic *P*-cell and the orthorhombic *C*-cell is the presence of weak superstructure reflections $d_{031} \approx 5.04$ Å and $d_{021} \approx 6.16$ Å which cannot be indexed in orthorhombic symmetry (Pažout et al. 2001). These reflections were frequently observed (Fig. 1) if enough sample was available for P-XRD experiments. Unit-cell parameters of Sb-rich gustavite (Pažout and Dušek 2009) and terrywallaceite (Yang et al. 2013) – last two lines in Tab. 1 – illustrate that with the Sb content rising, c and β increase while a and b parameters decrease. A distinctive negative correlation between gustavite substitution percentage and b parameter was noticed by Makovicky and Karup-Møller (1977b). However, such a correlation was not found in Kutná Hora samples. The reasons are multiple substitutions and the fact that – as

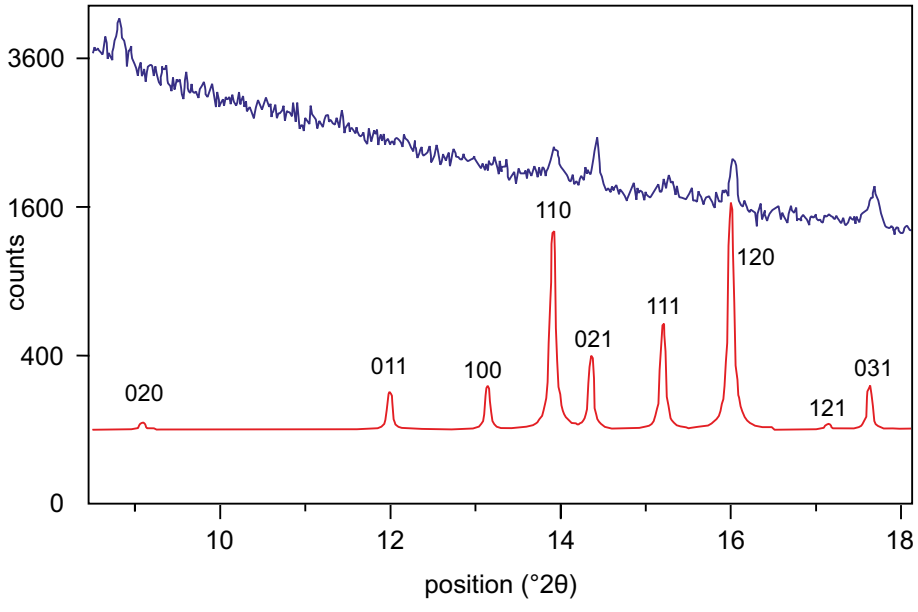

Fig. 1 Comparison of the low-angle part of the P-XRD pattern of terrywallaceite (sample ST 63-top) with a theoretical pattern calculated from the structure determined from the same sample (bottom) (Pažout and Dušek 2009). Reflections (020), (011), (100) have not been observed in gustavite powder patterns measured on laboratory diffractometers. CuK_α radiation.

Tab. 1 Refined unit-cell parameters of gustavite and terrywallaceite for the space group $P2_1/c$

Sample	Mineral	*a* [Å]	*b* [Å]	*c* [Å]	*β* [°]	*V* [Å³]	N_{chem}	L%	Bi/(Bi + Sb)
Gus[1)]	gustavite	7.064(1)	19.627(4)	8.211(2)	107.20(2)	1087.5	4.01	99.70	0.88
ST 37	gustavite	7.056(5)	19.599(10)	8.207(5)	107.16(5)	1084.5	3.99	86.46	0.81
ST 74	gustavite	7.057(5)	19.635(13)	8.213(5)	107.14(1)	1087.5	3.82	101.00	0.95
ST 29	terrywallaceite	7.068(6)	19.612(14)	8.216(7)	107.29(6)	1087.4	3.98	93.71	0.60
ST 61	terrywallaceite	7.056(9)	19.592(14)	8.235(9)	107.34(8)	1086.6	3.95	92.80	0.66
Sb Gus[2)]	terrywallaceite	7.0455(6)	19.5294(17)	8.3412(1)	107.446(10)	1094.9	4.02	107.70	0.69
Ter [3)]	terrywallaceite	6.9764(4)	19.3507(10)	8.3870(4)	107.519(2)	1079.7	3.94	106.35	0.49

[1)] unit-cell parameters refined from powder diffraction data (Pažout et al. 2001)
[2)] parameters refined from single-crystal diffraction data (Pažout and Dušek 2009)
[3)] parameters refined from single-crystal diffraction data (Yang et al. 2013)

seen in BSE images – even a small fragment extracted for powder diffraction is a mixture of several mineral phases. Cell parameters of several gustavite and terrywallaceite samples are in Tab. 1. The comparison of the low-angle part of the powder pattern of terrywallaceite with the theoretical one calculated from the crystal structure data (Pažout and Dušek 2009) is in Fig. 1.

Gustavite (L% = 60–109, Bi/(Bi + Sb) > 0.75, monoclinic). Chemical compositions of 96 samples (*c*. 350 point analyses) were identified as gustavite (members of gustavite–lillianite solid solution). The N_{chem} values are 3.79–4.29 (average 4.02); the substitution percentage L% ranges from 60 % (Gus_{60}), characterized by the formula $Ag_{0.64}Pb_{1.80}(Bi_{2.29}Sb_{0.26})_{\Sigma=2.55}S_{5.98}$, to 109 % ($Gus_{109}$), corresponding to $Ag_{1.04}Pb_{0.836}(Bi_{2.21}Sb_{0.95})_{\Sigma=3.16}S_{6.06}$. No analyses with L% < 50 % were found. No compositional gap between 60 and 113 % was observed; analysed points display a continuous solid solution (Fig. 2). At the same time, it should be noted that the majority of analyses fall between Gus_{90} and Gus_{100}. Gustavite compositions can be divided into three groups according the degree of Ag + Bi ↔ 2 Pb substitution (Tab. 2):

(1) Oversubstituted gustavite $Gus_{101–108.4}$ is rarer than terrywallaceite which is characterized by a similar substitution percentage but higher Sb content. It was identified in ten samples. It is also characterized by a high Sb content (Bi/(Bi + Sb) = 0.80–0.92). No Sb-free or Sb-poor oversubstituted gustavite was found.

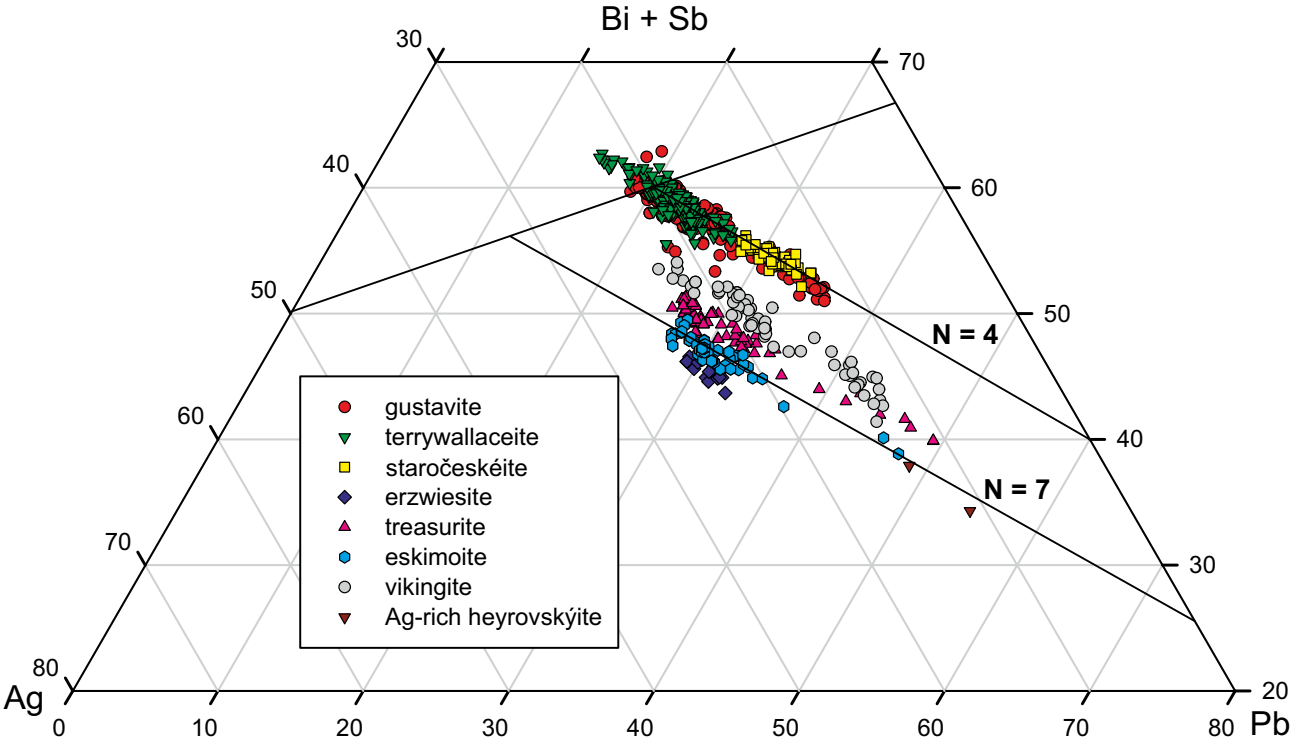

Fig. 2 Ternary diagram of the system Ag_2S–(Bi_2S_3 + Sb_2S_3)– PbS showing the $Ag^+ + (Bi,Sb)^{3+} \leftrightarrow 2Pb^{2+}$ substitution in lillianite homologues with Bi > Sb from Kutná Hora (*all analytical points plotted*). Five groups are present: (1) gustavite–lillianite solid solution, N = 4 (gustavite, terrywallaceite, staročeskéite), (2) vikingite solid solution, N = 5.5, (3) treasurite solid solution, N = 6, (4) eskimoite and heyrovskýite solid solutions, N = 7, and (5) erzwiesite, N = 8.

Tab. 2 Typical chemical analyses of gustavite (Bi/(Bi + Sb) > 0.75)

Sample	ST 140A2	ST 52gr1	ST 74fr1	ST 23Cgr1	ST 40Bgr1	ST 20gr1	ST 40Bgr1	ST 67Bgr1	ST 110A	ST 13B
n	4	2	3	9	2	4	5	3	2	5
Phase	Gus_{95}	Gus_{94}	Gus_{101}	Gus_{98}	Gus_{89}	Gus_{71}	Gus_{94}	Gus_{88}	Gus_{93}	Gus_{69}
Cu	0.00	0.00	0.00	0.01	0.02	0.00	0.00	0.01	0.02	0.00
Ag	8.96	9.06	9.18	9.16	8.93	6.89	9.09	8.66	9.37	6.48
Fe	0.22	0.06	0.00	0.02	0.34	0.01	0.01	0.02	0.03	0.04
Pb	19.14	19.74	18.82	19.27	20.78	27.78	20.74	23.14	21.66	29.2
Cd	0.18	0.1	0.09	0.09	0.11	0.12	0.04	0.05	0.04	0.13
Bi	53.12	52.02	53.5	52.13	50.69	43.43	45.39	43.97	45.1	43.5
Sb	0.96	1.02	1.79	1.98	1.91	3.01	5.8	6.22	6.97	3.32
Se	0.07	0.04	0.07	0.07	0.01	0.04	0.08	0.09	0.08	0.05
S	17.19	17.26	17.56	17.33	17.37	16.76	17.82	17.86	18.25	17.1
Total	99.85	99.31	101.01	100.05	100.14	98.05	98.97	100.03	101.51	99.81
Cu	0.00	0.00	0.00	0.00	0.00	0.00	0.00	0.00	0.00	0.00
Ag	0.93	0.94	0.94	0.95	0.92	0.74	0.92	0.87	0.92	0.68
Fe	0.05	0.01	0.00	0.00	0.07	0.00	0.00	0.00	0.01	0.01
Pb	1.04	1.07	1.00	1.04	1.11	1.54	1.09	1.21	1.11	1.59
Cd	0.02	0.01	0.01	0.01	0.01	0.01	0.00	0.01	0.00	0.01
Bi	2.85	2.80	2.83	2.78	2.69	2.39	2.37	2.29	2.29	2.36
Sb	0.09	0.09	0.16	0.18	0.17	0.28	0.52	0.55	0.61	0.31
Se	0.01	0.01	0.01	0.01	0.00	0.00	0.01	0.01	0.01	0.01
S	6.02	6.06	6.05	6.03	6.02	6.02	6.07	6.05	6.04	6.03
N_{chem}	3.95	4.06	3.82	3.92	4.12	4.12	3.98	4.02	4.01	4.00
L%	95.22	94.10	100.63	97.81	89.37	71.44	94.25	87.99	93.29	68.54
x	0.93	0.97	0.92	0.94	0.95	0.76	0.93	0.89	0.94	0.69
Bi/(Bi + Sb)	0.97	0.97	0.95	0.94	0.94	0.89	0.82	0.80	0.79	0.88

empirical formula coefficients based on 11 *apfu*
n – number of point analyses; *x* – substitution coefficient of the Ag + Bi ↔ 2 Pb substitution calculated as *x* = L% × (N – 2)/200 according to Makovicky and Karup-Møller (1977a)
analyses are ordered according to the increasing Sb contents

(2) "Normal" gustavite $Gus_{85–100}$ is the most frequent (320 point analyses, average N = 4.01 and Bi/(Bi + Sb) = 0.86). The samples richest in Bi have the composition $Gus_{90–98}$ (Fig. 3). Samples with the same Ag + Bi ↔ 2 Pb substitution range (L% = 85–100) but with even a higher Sb content corresponding to Bi/(Bi + Sb) < 0.75 are terrywallaceite.

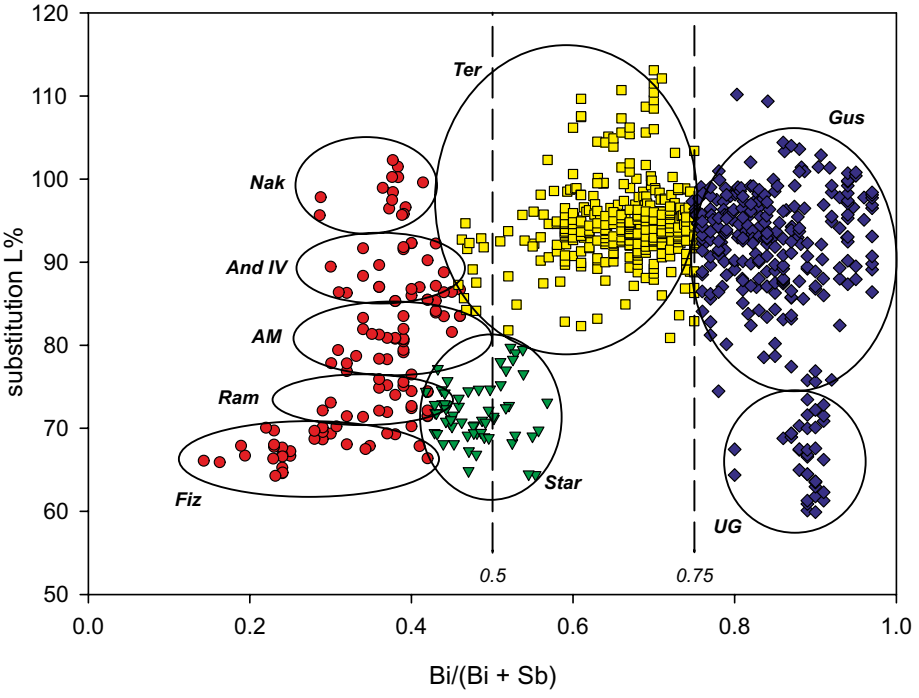

Fig. 3 The Bi/(Bi + Sb) (at. %) vs. Ag^{+} + $(Bi,Sb)^{3+}$ ↔ 2 Pb^{2+} substitution (L%) plot of all lillianite homologues with N = 4. Red circles – andorite branch minerals with N = 4: Fiz – fizelyite, Ram – ramdohrite, AM – mixture of fine exsolution lamellae of several andorite phases (And IV, Ram, Fiz), And IV – andorite IV (quatrandorite), Nak – Cu-bearing andorite VI (nakaséite); green triangles – staročeskéite (Star) with Bi/(Bi + Sb) ~ 0.5 and L% from 65 to *c.* 77; yellow squares – terrywallaceite (Ter); blue diamonds – gustavite (Gus), UG – undersubstituted gustavite $Gus_{60–75}$ (probably representing a mixture of fine exsolution lamellae of gustavite and lillianite). The plot shows that most undersubstituted gustavite points have low Sb contents. Oversubstituted points are Sb-rich and belong to terrywallaceite. It is also evident that most gustavite and terrywallaceite analyses have L% between 85 and 100 with a complete substitution of Sb for Bi (Bi/(Bi + Sb) = 0.51–0.97).

(3) Undersubstituted gustavite $Gus_{60–85}$. Although a miscibility gap was proposed to exist between Gus_{55} and Gus_{85} (Makovicky and Karup-Møller 1977b), points with this composition were found in 57 analyses. They are characterized by relatively low Sb contents with average Bi/(Bi + Sb) of 0.86. Crystal structure of one such sample (ST 163, chemically Gus^{91}_{71}) was measured by a single-crystal XRD. The symmetry was found to be compatible with monoclinic $P2_1/c$ gustavite cell but it could not be refined to R_{obs} factor better than *c.* 15 %. This is caused most probably by an intergrowth of gustavite and lillianite slabs (Makovicky, pers. comm.).

Terrywallaceite (L% = 85–113, Bi/(Bi + Sb) < 0.75, monoclinic) was described by Yang et al. (2013) from Peru, although it was found before in Kutná Hora ore district and its structure was solved by Pažout and Dušek (2009). Its crystal structure is the same as that of Sb gustavite (Pažout and Dušek 2009): it also contains three mixed Bi + Sb sites, of which two, sites M1 and M2, display Bi > Sb occupancy and M3 has Sb > Bi. The only difference is that the occupancy of Sb in M3 site of terrywallaceite from Peru is 0.95 (corresponding to Bi/(Bi + Sb) = 0.49) and that of Sb gustavite from Kutná Hora is 0.65 (corresponding to Bi/(Bi + Sb) = 0.69). Given that both show Sb > Bi in M3 site and both have the $P2_1/c$ unit cell of gustavite, they constitute the same mineral species. Yang et al. (2013) concluded that both terrywallaceite and Sb-rich gustavite of Pažout and Dušek (2009) display the same preference of Sb for the M3 site over M2 and M1 sites. Thus, the occupancy of Sb at the M3 site will exceed that of Bi when the Bi/(Bi + Sb) ratio is only *c.* 75 %. The correct structural formula for terrywallaceite is then $AgPb(Sb,Bi)(Bi,Sb)_2S_6$. Antimony-rich oversubstituted gustavite, $Ag_{1.08}Pb_{0.84}(Bi_{2.11}Sb_{0.96})(S_{5.93}Se_{0.01})$, investigated by Pažout and Dušek (2009), is thus positioned in the terrywallaceite compositional field. Therefore, all oversubstituted samples (L% > 100) with Bi/(Bi + Sb) between 0.50 and 0.75 are terrywallaceite.

Tab. 3 Typical chemical analyses of terrywallaceite (Bi/(Bi + Sb) = 0.50–0.75)

Sample	ST 78	ST 63A	ST 186A	ST 78	ST 23Cr	ST 22E
n	3	12	11	4	5	5
Phase	Ter_{98}	Ter_{108}	Ter_{98}	Ter_{93}	Ter_{105}	Ter_{91}
Cu	0.01	0.00	0.04	0.01	0.02	0.10
Ag	10.05	11.36	10.28	10.13	10.35	9.80
Fe	0.01	0.01	0.01	0.00	0.02	0.00
Pb	20.56	16.90	20.66	22.31	18.49	23.54
Cd	0.01	0.01	0.00	0.01	0.03	0.00
Bi	43.39	42.98	39.46	38.21	39.82	32.55
Sb	9.41	11.39	11.84	12.25	12.53	15.66
Se	0.10	0.08	0.00	0.07	0.21	0.00
S	18.15	18.51	18.82	18.53	18.67	19.09
Total	101.67	101.23	101.12	101.52	100.13	100.78
Cu	0.00	0.00	0.01	0.00	0.00	0.02
Ag	0.98	1.09	0.98	0.97	0.99	0.92
Fe	0.00	0.00	0.00	0.00	0.00	0.00
Pb	1.04	0.84	1.03	1.11	0.92	1.15
Cd	0.00	0.00	0.00	0.00	0.00	0.00
Bi	2.19	2.13	1.94	1.89	1.97	1.58
Sb	0.81	0.97	1.00	1.04	1.06	1.30
Se	0.01	0.01	0.00	0.01	0.03	0.00
S	5.96	5.96	6.04	5.97	6.02	6.03
N_{chem}	3.99	4.02	4.07	4.13	3.87	4.11
L%	98.12	107.72	97.62	93.48	104.75	91.35
x	0.97	1.09	1.01	1.00	0.98	0.96
Bi/(Bi + Sb)	0.73	0.69	0.66	0.65	0.65	0.55

empirical formula coefficients based on 11 *apfu*
n – number of point analyses
x – substitution coefficient of the Ag + Bi = 2Pb substitution
the number past the phase symbol is the substitution percentage L%
analyses are ordered according to the increasing Sb contents

Terrywallaceite was found in 67 samples (330 analytical points). It is characterized by high Sb content (Bi/(Bi + Sb) = 0.50–0.75; mean 0.67) and substitution between 85 and 113 % ($Ter_{85.4–113.1}$) (Tab. 3, Electronic Supplementary Material 1). Crystal structure of one such sample (ST 63) was solved and discussed by Pažout and Dušek (2009), even though the mineral was called Sb-rich gustavite in that paper. The formula of this sample based the microprobe data is $Ag_{1.08}Pb_{0.84}(Bi_{2.11}Sb_{0.96})$ $(S_{5.93}Se_{0.01})$, Z = 4, N_{chem} = 4.02, Bi/(Bi + Sb) = 0.69 and gustavite substitution L = 107.2 %.

Staročeskéite (L% = 65–75, Bi/(Bi + Sb) ≈ 0.50, orthorhombic) is a new, recently approved mineral (IMA No. 2016–101) of the lillianite homologous series with N = 4. Homogeneous grains of this phase up to several hundred microns across were observed, associated with other lillianite homologues and Ag,Bi-rich galena (Fig. 4). The empirical formula calculated from EMP analysis of the sample ST 37, in which the mineral was determined and described, is $Ag_{0.69}Pb_{1.56}(Bi_{1.32}Sb_{1.37})_{\Sigma=2.69}$ $(S_{6.04}Se_{0.01})_{\Sigma6.05}$ corresponding to N_{chem} = 3.94, Bi/(Bi + Sb) = 0.49 and L% = 70.5 (Tab. 4). The formula based

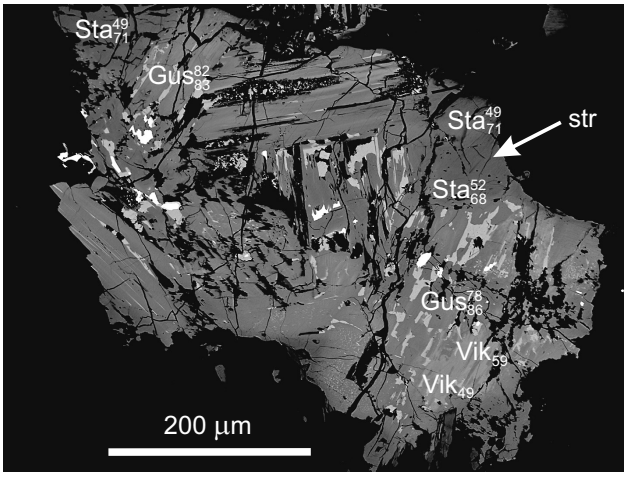

Fig. 4 Gustavite $Gus_{83–86}$, vikingite $Vik_{49–59}$ and staročeskéite Sta^{49}_{71} and Sta^{52}_{68}. BSE image of sample ST 37. A fragment for single-crystal XRD analysis of staročeskéite was extracted from the spot marked by the arrow ("str").

on crystal structure data – $Ag_{0.71}Pb_{1.52}(Bi_{1.32}Sb_{1.45})_{\Sigma=2.69}S_6$ – agrees well with that derived from chemical data (Pažout and Dušek 2010). The mineral is of orthorhombic symmetry, space group *Cmcm*, with a = 4.2539(8), b = 13.3094(8), c = 19.625(1) Å, V = 1111.1(2) Å^3, Z = 4. Its composition falls between two gaps in two series (lillianite and andorite series) and might exist only because of the Bi-Sb mixing 1 : 1. The mineral represents a new *homeotype* from gustavite–andorite extended series of lillianite-type structures with N = 4 (Makovicky pers.comm.).

Seventeen samples (36 microprobe analyses) with average Bi/(Bi + Sb) = 0.50 (sample means vary between 0.43 and 0.56) and substitution around 70 % belong to staročeskéite. Chemically they can be classified as transitional between end-members of gustavite–lillianite series and andorite group minerals. The inferred succession of associated minerals was: galena → vikingite → gustavite → staročeskéite, with Sb contents increasing over the time.

Tab. 4 Typical chemical analyses of staročeskéite

Sample	ST 37	ST 70C	ST 90A	ST 25gr1
n	5	5	3	7
Phase	Sta70	Sta68	Sta70	Sta72
Cu	0.05	0.05	0.02	0.05
Ag	7.02	6.68	7.23	7.71
Fe	0.05	0.05	0.05	0.08
Pb	31.09	31.30	31.27	30.57
Cd	0.10	0.05	0.19	0.03
Bi	26.62	29.05	27.17	24.18
Sb	16.01	13.58	15.77	17.63
Se	0.07	0.05	0.06	0.06
S	18.66	18.20	18.87	18.80
Total	99.67	99.00	100.63	99.11
Cu	0.01	0.01	0.00	0.01
Ag	0.68	0.66	0.69	0.74
Fe	0.01	0.01	0.01	0.01
Pb	1.56	1.61	1.55	1.52
Cd	0.01	0.00	0.02	0.02
Bi	1.32	1.48	1.34	1.19
Sb	1.37	1.19	1.33	1.49
Se	0.01	0.01	0.01	0.01
S	6.04	6.04	6.05	6.03
N_{chem}	3.94	3.95	4.00	4.12
L%	70.46	68.18	70.09	72.40
x	0.68	0.67	0.70	0.95
Bi/(Bi + Sb)	0.49	0.55	0.50	0.44

empirical formula coefficients based on 11 *apfu*
n – number of point analyses
x – substitution coefficient of the Ag + Bi ↔ 2 Pb substitution

Trends within multicompositional grains of minerals with N = 4, i.e. those featuring three or more different gustavite, terrywallaceite, staročeskéite or andorite

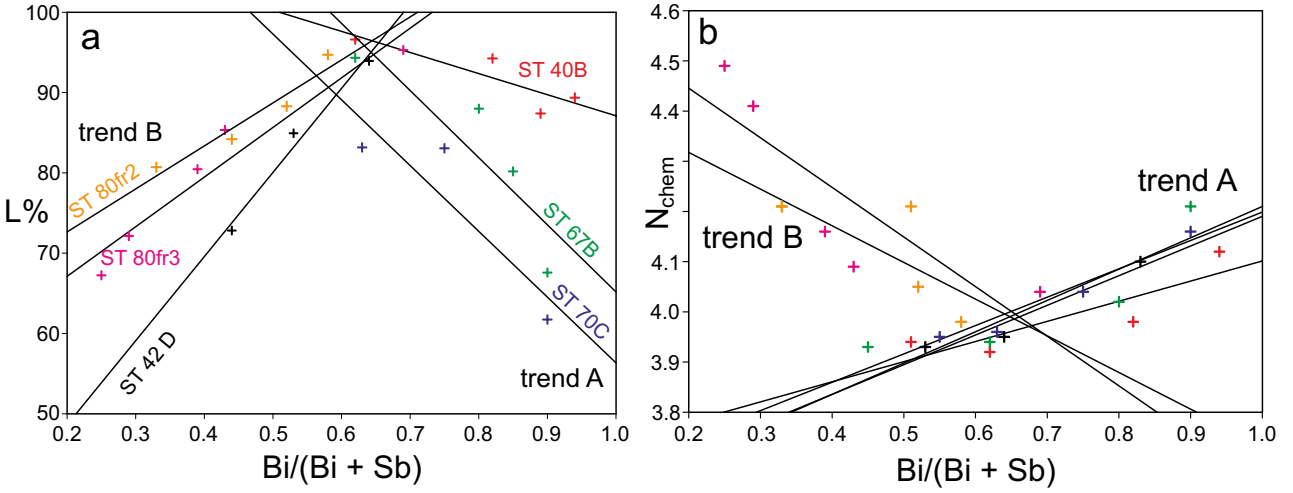

Fig. 5 Trends within multicompositional grains of gustavite and andorite. **a** – Bi/(Bi + Sb) in at. % vs. L%: negative correlation (trend A) is typical of gustavite and positive one (trend B) of andorite. **b** – Bi/(Bi + Sb) in at. % vs. N_{chem}: positive correlation (trend A) is typical of gustavite, negative one (trend B) of andorite.

Tab. 5 Trends observed within multicompositional grains of minerals with N = 4

	Sb	L%	N_{chem}	Typical of
trend A	↑	↑	↓	gustavite (Bi > Sb)
trend B	↑	↓	↑	andorite (Sb > Bi)
trend C	↑	→	→	
trend D	↑	↑	→	

↑ – increasing value; ↓ – decreasing value; → no change

compositions within one grain with no apparent grain boundary. Two major and several weak trends have been observed in analyzed samples relating the extent of the Ag + Bi ↔ 2 Pb substitution, N_{chem} and Sb contents within individual multicompositional grains (Tab. 5). Trend A displays increase in Sb content (↑) accompanied by the L% increase (↑) and N_{chem} decrease (↓); trend B shows Sb ↑, L% ↓, N ↑; trend C – with Sb ↑, L% and N invariant (→) and trend D – with Sb ↑, L% ↑, N →. Trend A is the most frequently encountered and is typical of gustavite and terrywallaceite (Bi > Sb) single grains (Fig. 5). There is a positive correlation between Sb content and the extent of gustavite substitution (oversubstituted gustative is Sb-rich), simultaneously accompanied by the decrease of N. Trend B is also common and it is typical of andorite (Sb > Bi) single grains (Fig. 5). It is an opposite of the trend A, with L% decreasing with increasing Sb (fizelyite is poorer in Bi than quatrandorite), accompanied by the increase of N. Trends C and D are less frequent.

Another feature frequently observed in the Kutná Hora samples is a transition from Bi- to Sb-dominant phases (from gustavite to andorite) (Fig. 6) from centre to the rim of the grains (Fig. 7a). An example of compositional variations of gustavite within a single grain is shown in the sample ST 40Bgr1 (Fig. 7b, Tab. 6). Within one grain (11 point analyses), five different compositions were detected: Bi/(Bi + Sb) ratio changes from 0.95 (almost Sb-free gustavite with only 1.61 wt. % of Sb, or 2.96 mol. % Sb_2S_3) to 0.51 (terrywallaceite with 28.9 mol. % Sb_2S_3) while the N and L% values remain within a narrow range (N = 3.92–4.18, L% = 87.1–98.1), following the trend A. The BSE image of the sample appears homogenous with a few blurred spots of a darker shade of grey (which represent terrywallaceite) with no apparent grain boundary. Very good examples of multicompositional grains of various lillianite homologues with N = 4 are samples ST 42Dgr1, ST 80fr2 and ST 90A in Electronic Supplementary Material 1.

A weak positive correlation between Sb content and extent of gustavite substitution (without reflecting N_{chem} values) was observed by Cook (1997) and the same positive correlation between N and L% (without reflecting Sb content) by Makovicky and Karup-Møller (1977b) in oversubstituted gustavite.

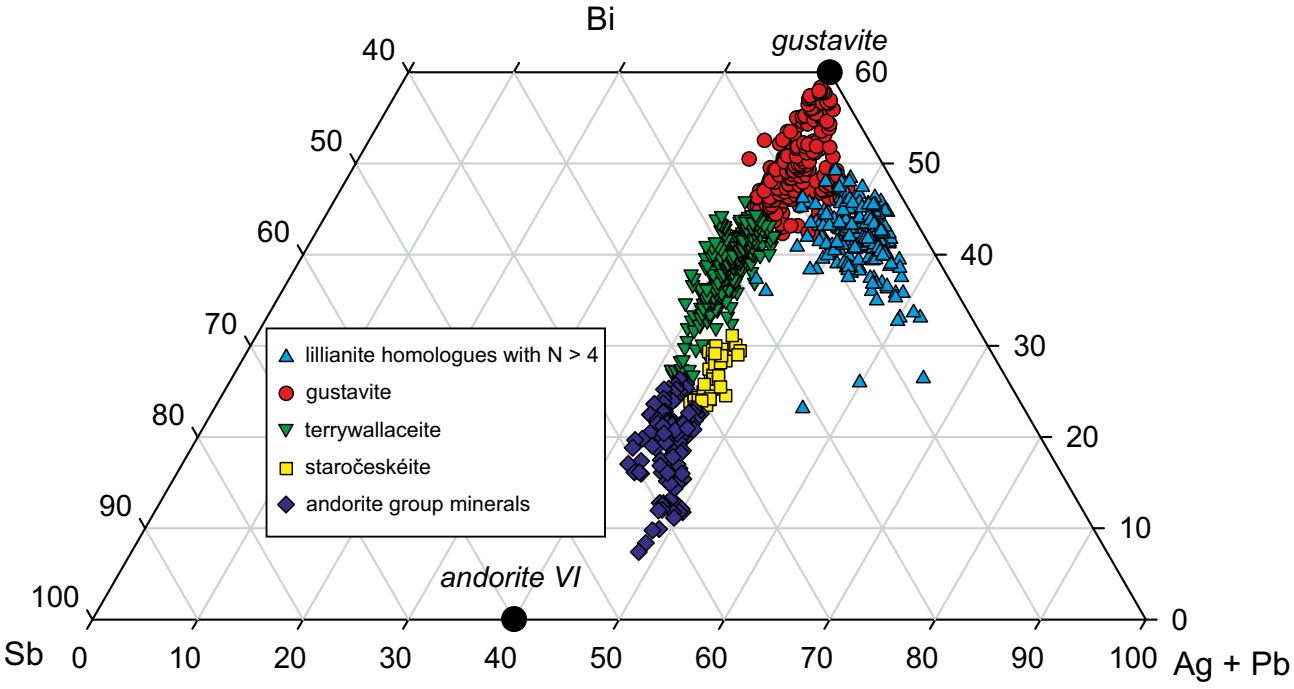

Fig. 6 Ternary diagram of the system Sb_2S_3–Bi_2S_3–(Ag_2S + PbS) for all lillianite homologues from Kutná Hora. Cluster of compositions along the $AgPbSb_3S_6$–$AgPbBi_3S_6$ join shows continuous Bi^{3+} ↔ Sb^{3+} field of substitution from Bi/(Bi + Sb) = 0.97–0.23 (corresponding to 3–73 % of Bi substituted by Sb). Plot demonstrates that higher lillianite homologues (N > 4) have only a very limited substitution of Sb for Bi.

Tab. 6 An example of analyses of multicompositional grains of lillianite homologues with N = 4 (several compositions within one grain differing by L%, Sb content or both)

Sample	ST 40Bgr1					ST 70C				ST 80fr3					ST 89B			
n	2	2	5	2	1	9	4	1	5	5	1	2	1	1	3	2	1	2
Phase	Gus_{89}	Gus_{87}	Gus_{94}	Ter_{97}	Ter_{93}	Gus_{62}	Gus_{83}	Ter_{83}	Sta_{68}	Ter_{95}	And_{85}	And_{92}	And_{80}	And_{72}	Sta_{73}	And_{69}	And_{71}	And_{66}
Cu	0.02	0.01	0.00	0.02	0.00	0.01	0.01	0.03	0.05	0.01	0.05	0.04	0.06	0.10	0.04	0.01	0.01	0.03
Ag	8.93	8.81	9.09	9.41	9.62	6.06	8.24	8.36	6.68	10.01	9.39	10.19	9.13	8.70	7.96	7.48	7.95	7.68
Fe	0.34	0.05	0.01	0.02	0.01	0.01	0.02	0.05	0.05	0.01	0.19	0.02	0.04	0.06	0.05	0.04	0.06	0.08
Pb	20.78	22.47	20.74	20.75	23.34	31.67	25.14	26.13	31.30	21.61	25.93	24.68	28.63	32.16	31.6	32.77	32.42	35.49
Cd	0.11	0.05	0.04	0.01	0.12	0.10	0.05	0.00	0.05	0.00	0.00	0.00	0.16	0.19	0.01	0.03	0.07	0.12
Bi	50.69	47.19	45.39	35.92	30.57	42.13	40.60	35.56	29.05	40.67	25.40	24.12	23.03	16.22	24.28	20.67	19.3	13.75
Sb	1.91	3.44	5.80	12.71	17.25	2.81	7.79	12.02	13.58	10.85	19.87	22.40	21.04	23.57	18.91	20.21	21.83	24.82
Se	0.01	0.11	0.08	0.09	0.14	0.05	0.06	0.11	0.05	0.08	0.04	0.04	0.07	0.05	0.07	0.04	0.03	0.06
S	17.37	17.46	17.82	18.37	19.26	17.00	17.82	18.53	18.20	18.17	17.82	19.18	19.21	18.73	18.78	18.61	18.75	19.15
Total	100.14	99.59	98.97	97.30	100.31	99.83	99.74	100.79	99.00	101.41	98.68	100.66	101.37	99.78	101.68	99.85	100.43	101.16
Cu	0.00	0.00	0.00	0.00	0.00	0.00	0.00	0.00	0.01	0.00	0.03	0.02	0.04	0.06	0.02	0.00	0.01	0.02
Ag	0.92	0.91	0.92	0.92	0.90	0.64	0.83	0.81	0.66	0.97	3.62	3.73	3.36	3.24	2.99	2.84	2.98	2.81
Fe	0.07	0.01	0.00	0.00	0.00	0.00	0.00	0.01	0.01	0.00	0.14	0.01	0.03	0.04	0.03	0.03	0.05	0.06
Pb	1.11	1.20	1.09	1.06	1.13	1.74	1.32	1.32	1.61	1.09	5.21	4.71	5.48	6.23	6.18	6.48	6.32	6.77
Cd	0.01	0.01	0.00	0.00	0.01	0.01	0.00	0.00	0.00	0.00	0.00	0.00	0.06	0.07	0.00	0.01	0.02	0.04
Bi	2.69	2.51	2.37	1.82	1.47	2.30	2.11	1.78	1.48	2.04	5.06	4.57	4.37	3.12	4.71	4.05	3.73	2.60
Sb	0.17	0.31	0.52	1.10	1.43	0.26	0.69	1.03	1.19	0.93	6.79	7.28	6.86	7.77	6.29	6.80	7.25	8.06
Se	0.00	0.02	0.01	0.01	0.02	0.01	0.01	0.01	0.01	0.01	0.02	0.02	0.04	0.03	0.03	0.02	0.02	0.03
S	6.02	6.04	6.07	6.07	6.04	6.04	6.03	6.04	6.04	5.95	23.12	23.65	23.77	23.45	23.73	23.77	23.63	23.61
N_{chem}	4.12	4.18	3.98	3.92	3.94	4.16	4.04	3.96	3.95	4.04	4.09	4.03	4.16	4.41	4.06	4.05	4.10	4.21
L%	89.37	87.40	94.25	96.60	92.52	61.74	83.06	83.17	68.18	95.30	85.34	91.67	80.45	72.13	73.05	69.33	71.37	65.71
x	0.95	0.95	0.93	0.93	0.90	0.67	0.85	0.82	0.67	0.97	0.89	0.93	0.87	0.87	0.75	0.71	0.75	0.73
Bi/(Bi + Sb)	0.94	0.89	0.82	0.62	0.51	0.90	0.75	0.63	0.55	0.69	0.43	0.39	0.39	0.29	0.43	0.37	0.34	0.24

phases with Bi/(Bi + Sb) < 0.50 are labelled andorite (And) and based on 44 *apfu*
the means of the analyses of the same composition within each grain (n is the number of measured points) are ordered from the highest Bi/(Bi + Sb) ratio to the lowest
empirical formula coefficients of gustavite (Gus), terrywallaceite (Ter) and staročeskéite (Sta) based on 11 *apfu*
for andorite branch minerals on 44 *apfu* (And_{92} – Bi-rich andorite IV, And_{72} – Bi-rich ramdohrite, And_{80} represents a submicroscopic intergrowth of two Bi-rich andorite phases)
n – number of point analyses; *x* – substitution coefficient of the Ag + Bi ↔ 2 Pb substitution

4.1.2. Lillianite homologues with $N_{chem} > 4$

Vikingite, treasurite and eskimoite were identified chemically and confirmed by P-XRD. Schimerite, heyrovskýite and erzwiesite were identified on the basis of the chemical composition only. Chemistry of all identified Ag–Bi lillianite homologues with N > 4 (including schirmerite) exhibits one distinct feature: only limited (much lower than for minerals with N = 4) and fairly constant Sb content, never exceeding *c.* 5 at. %. Unlike in members with N = 4, no continuous transition to Sb-dominant phases of the same N_{chem} and L% has been found. It was observed that all higher lillianite homologues (with N > 4) are always accompanied by gustavite or terrywallaceite. The succession of crystallization was as follows: native Bi → Ag,Pb-rich $galena_{ss}$ → lillianite homologues with N > 4 → lillianite homologues with N = 4 → Sb-rich gustavite → terrywallaceite → staročeskéite → Bi-rich andorite minerals → Bi-rich Pb–Sb sulphosalts (Bi-rich jamesonite, Bi-rich boulangerite). The Sb-richest minerals crystallized at the final stage.

Vikingite ($^{4,7}L$, N_{chem} = 5.5) is rare and forms elongated grains (laths, lamellae), usually under 200 μm long, in quartz, intergrown or associated with other lillianite homologues and galena (Fig. 7c). It always occurs with gustavite or terrywallaceite from which it may distinguished by a lighter shade of grey in BSE images. However, it cannot be discerned from treasurite, eskimoite or cosalite. It is the first occurrence reported from the Czech Republic.

Twenty-one samples (57 point analyses) were identified as members of the vikingite solid solution. Average N_{chem} for all points is 5.42 (averages for individual samples vary between 5.25 and 5.56). The

Tab. 7 Chemical analyses of vikingite

Sample	ST 20gr1	ST 23Bfr1	ST 37	ST 42Cgr1	ST 42Cgr2	ST 42Dgr1	ST 55gr2	ST 70C	ST 71Afr1	ST 62	ST 85 gr1	ST 84A	ST 103gr1top	ST 11A
n	3	4	5	3	2	4	2	2	7	2	4	2	2	1
Phase	Vik_{50}	Vik_{67}	Vik_{51}	Vik_{68}	Vik_{68}	Vik_{69}	Vik_{53}	Vik_{48}	Vik_{70}	Vik_{66}	Vik_{70}	Vik_{76}	Vik_{53}	Vik_{85}
Cu	0.02	0.00	0.02	0.02	0.03	0.01	0.00	0.02	0.01	0.00	0.01	0.06	0.13	0.07
Ag	6.09	8.64	6.54	9.13	8.84	8.94	6.67	5.92	8.88	8.78	9.28	9.61	6.46	11.43
Fe	0.01	0.13	0.02	0.03	0.00	0.01	0.01	0.01	0.01	0.02	0.01	0.06	0.03	0.00
Pb	37.99	30.41	38.31	31.00	31.00	29.55	36.71	39.7	29.42	31.57	29.94	26.79	36.44	22.66
Cd	0.15	0.07	0.09	0.13	0.08	0.08	0.13	0.10	0.10	0.09	0.12	0.06	0.15	0.07
Bi	37.28	36.73	34.63	40.25	39.44	39.74	37.86	34.6	38.54	42.96	40.74	44.01	34.24	39.86
Sb	2.01	5.76	3.74	4.05	4.38	3.75	1.97	3.97	5.14	1.35	3.96	3.11	4.57	7.21
Se	0.11	0.06	0.07	0.09	0.10	0.09	0.05	0.03	0.08	0.08	0.05	0.00	0.02	0.00
S	16.12	16.94	16.54	17.13	17.07	16.91	16.29	16.39	17.28	16.92	17.07	17.48	16.09	17.63
Total	99.78	98.75	99.96	101.82	100.94	99.08	99.68	100.74	99.46	101.76	101.18	101.17	98.13	98.95
Cu	0.01	0.00	0.01	0.01	0.02	0.01	0.00	0.02	0.01	0.00	0.01	0.05	0.12	0.06
Ag	3.36	4.57	3.54	4.75	4.63	4.76	3.66	3.21	4.65	4.65	4.85	4.98	3.56	5.83
Fe	0.01	0.13	0.02	0.03	0.00	0.01	0.01	0.01	0.01	0.02	0.01	0.06	0.04	0.00
Pb	10.92	8.37	10.79	8.40	8.45	8.18	10.49	11.21	8.02	8.70	8.16	7.23	10.44	6.02
Cd	0.08	0.04	0.05	0.06	0.04	0.04	0.07	0.05	0.05	0.04	0.06	0.03	0.08	0.03
Bi	10.62	10.02	9.66	10.81	10.66	10.91	10.72	9.68	10.41	11.74	11	11.79	9.73	10.5
Sb	0.98	2.7	1.79	1.87	2.03	1.77	0.96	1.91	2.38	0.63	1.83	1.43	2.23	3.26
Se	0.08	0.05	0.05	0.06	0.07	0.06	0.04	0.02	0.06	0.06	0.04	0.00	0.01	0.00
S	29.93	30.12	30.08	30	30.08	30.26	30.06	29.89	30.42	30.15	30.04	30.5	29.8	30.27
N_{chem}	5.33	5.36	5.56	5.56	5.43	5.5	5.46	5.25	5.28	5.68	5.51	5.25	5.33	5.53
L%	49.52	67.27	50.89	67.76	67.56	69.08	52.77	47.68	70.02	65.51	69.72	75.7	53.46	84.94
x	0.82	1.13	0.9	1.21	1.16	1.21	0.91	0.78	1.14	1.2	1.22	1.23	0.89	1.50
Bi/(Bi + Sb)	0.92	0.79	0.84	0.85	0.84	0.86	0.92	0.84	0.81	0.95	0.86	0.89	0.81	0.76

empirical formula coefficients based on 56 *apfu*

n – number of point analyses; *x* – substitution coefficient of the Ag + Bi ↔ 2 Pb substitution

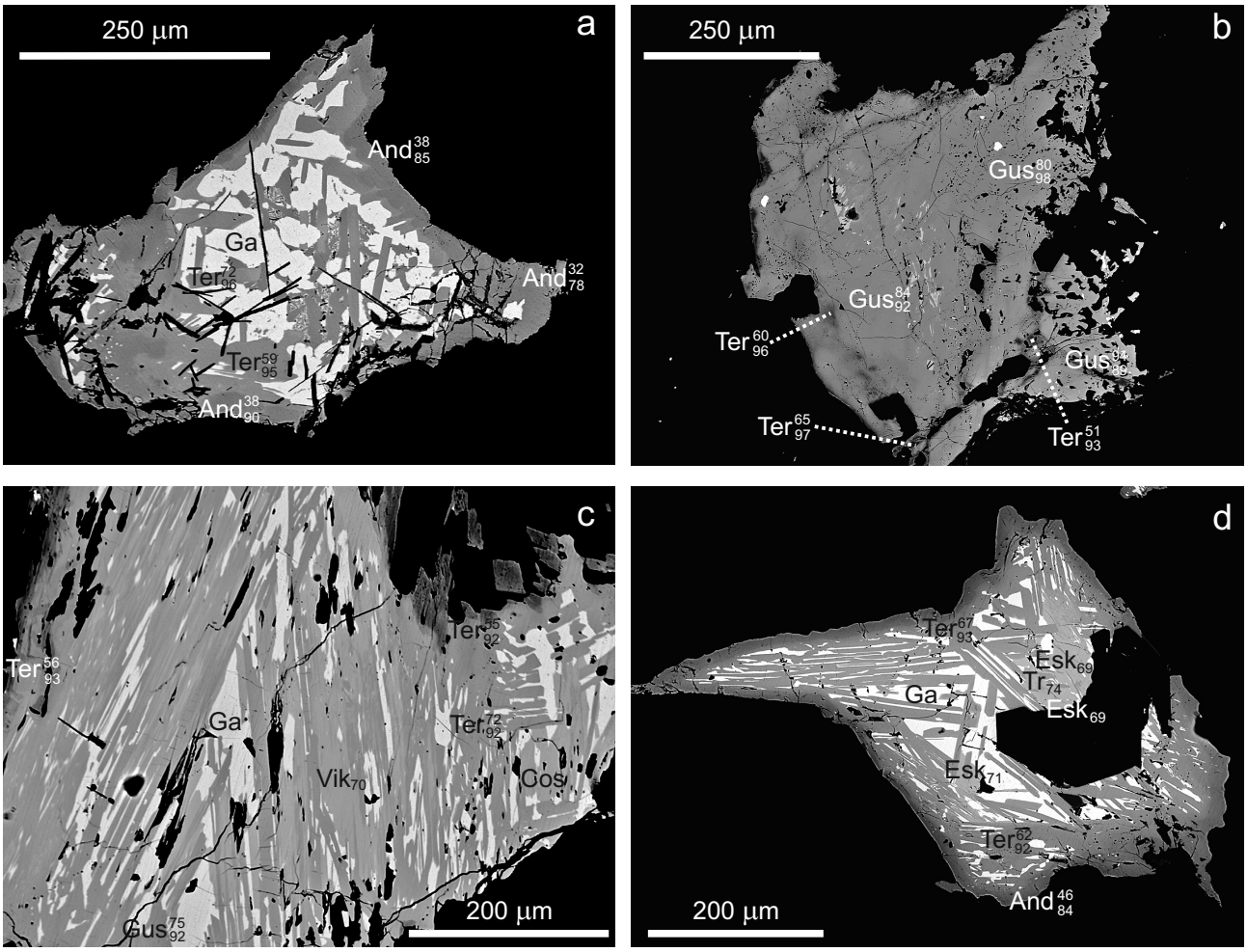

Fig. 7 Back-scattered electron images of lillianite homologues from Kutná Hora. **a –** A grain showing Sb-rich rim with three different andorite compositions, all with very similar Bi contents: Bi-rich ramdohrite (And_{78}), Bi-rich quatrandorite (And_{90}) and their intergrowth (And_{85}). The centre of the grain is formed by Ag,Bi-galena (Ga – white) and two compositions of terrywallaceite (Ter) with the same substitution percentage L% (95–96 %) but different Sb contents ((Bi/(Bi + Sb) = 0.72 (lighter grey) and 0.59). Sample ST 29. **b –** Relatively homogeneous gustavite grain (in terms of gustavite substitution) but with very variable Sb contents. Sample ST 40. **c –** Lamellar character of lillianite phases replacing galena. Gus – gustavite, Ter – terrywallaceite, Ga – galena solid solution, Vik – vikingite, Cos – cosalite; Sample ST 71A. **d** – Replacement of Ag,Bi--galena (Ga – white) by lillianite homologues: lath-shaped crystals of eskimoite $Esk_{69–71}$ and treasurite Tr_{74} in the centre, allotriomorphic grains of terrywallaceite ($Ter_{92–93}$) closer to the rim and darker, Sb-rich rim of the grain is formed by And_{84}. A trend of Sb enrichment from the lighter centre to the darker rim is clearly visible. Sample ST 61.

Ag + Bi ↔ 2 Pb substitution ranges from 46.7 % to 85 % ($Vik_{48–85}$). Vikingite from the type locality Ivigtut, Greenland, corresponds to $Vik_{60–67}$. Antimony content remains constant within grains and low if compared to gustavite. The ratio Bi/(Bi + Sb) = 0.75–0.95. Compositional ranges of all points determined as vikingite can be expressed as $^{5.02–5.88}Vik^{75–95}_{47–85}$.

Chemical compositions are plotted in Figs 2 and 6. With the increasing Ag + Bi ↔ 2 Pb substitution, the formulae (calculated to a total of 56 *apfu*) vary from $Ag_{3.34}Pb_{11.46}(Bi_{9.38}Sb_{1.65})_{\Sigma=11.03}S_{30.13}$, ($Vik_{48}$), to $Ag_{5.83}Pb_{6.02}(Bi_{10.50}Sb_{3.26})_{\Sigma=13.76}S_{30.27}$, ($Vik_{85}$), (Tab. 7). All samples are almost Cu-free. Of other detected elements, interesting is the content of Cd (max. 0.21 wt. %).

Tab. 8 Refined unit-cell parameters of vikingite from Kutná Hora for the space group C2/m in comparison with the structure (Makovicky et al. 1992)

Sample	*a* [Å]	*b* [Å]	*c* [Å]	*β* [°]	*V* [Å^3]	N_{chem}	L%	Bi/(Bi + Sb)
ST 20	13.59(2)	4.114(5)	25.18(3)	95.45(9)	1401.3	5.33	49.52	0.92
ST 37	13.57(1)	4.107(3)	25.27(2)	95.56(4)	1401.4	5.56	50.89	0.84
ST 42B	13.58(2)	4.123(8)	25.24(2)	95.34(2)	1406.9	5.50	68.13	0.85
Structure	13.598(3)	4.112(2)	25.249(7)	95.59(5)	1405.1		56.40	1.00

Vikingite was detected in the P-XRD patterns of five out of the nine samples measured on electron microprobe. Unit-cell parameters of vikingite were refined from powder data indexed in the space group *C*2/*m* (Makovicky et al. 1992) (Tab. 8). Small amounts of vikingite available were the cause of poorer quality of the P-XRD data. No attempt has been made to extract the grain for single-crystal diffraction from the polished section due to intimate intergrowth with gustavite.

Treasurite ($^{4,8}L$, N_{chem} = 6) is rarer than vikingite in Kutná Hora and always occurs with gustavite or terrywallaceite. It forms lamellae or grains up to 200 μm across. In BSE images it is undistinguishable from vikingite, eskimoite or cosalite (Fig. 7d). It is the first occurrence reported from the Czech Republic.

Treasurite was found in several parageneses, in all but two cases accompanied by vikingite. In the sample ST 32 it is part of light silvery grey grain aggregates up to 7 mm across, consisting of $Gus_{87–93}$ and minor galena, intergrown with massive pyrrhotite. In the sample ST 57 it forms mosaic-like lamellae in galena accompanied by Gus_{92}. There is no pyrrhotite in the sample and the character of the quartz gangue suggests low-temperature crystallization.

Twelve samples (36 point analyses) were identified to belong to the treasurite solid solution with the average N_{chem} = 6.06 (total range 5.74–6.43). Chemical compositions and empirical formulae (formula normalised to 60 atoms, Z = 1) are listed in Tab. 9 and plotted in Figs 2 and 6. The Ag + Bi ↔ 2 Pb substitution ranges from 38.4 % ($Tr_{38.4}$): $Ag_{3.01}Pb_{13.66}(Bi_{9.11}Sb_{1.94})_{\Sigma=11.04}S_{32.28}$ to 77.8 % ($Tr_{77.8}$): $Ag_{6.32}Pb_{7.30}(Bi_{12.41}Sb_{1.34})_{\Sigma=13.75}S_{32}$. Similar to other lil-

Tab. 9 Chemical analyses of treasurite

Sample	ST 32	ST 42Dgr1	ST 55gr2	ST 57gr2	ST 61gr1	ST 70C	ST 71Afr1	ST 10A	ST 126A2	ST103 gr1top	ST 126A2	ST 22D
n	3	1	2	2	2	2	1	1	2	2	1	3
Phase	Tr_{68}	Tr_{66}	Tr_{49}	Tr_{70}	Tr_{74}	Tr_{38}	Tr_{56}	Tr_{67}	Tr_{68}	Tr_{42}	Tr_{72}	Tr_{78}
Cu	0.01	0.02	0.01	0.00	0.01	0.03	0.02	0.09	0.00	0.03	0.00	0.01
Ag	9.63	8.94	6.43	10.43	10.50	5.05	7.96	9.27	9.67	5.52	10.12	11.26
Fe	0.02	0.02	0.02	0.00	0.06	0.01	0.00	0.05	0.16	0.00	0.12	0.02
Pb	30.11	31.78	39.05	29.99	28.12	44.31	36.14	31.15	29.64	41.58	27.28	24.96
Cd	0.12	0.08	0.08	0.15	0.07	0.07	0.13	0.08	0.19	0.28	0.19	0.00
Bi	42.31	38.02	34.73	37.86	39.83	29.94	33.53	39.00	41.90	32.43	42.94	42.83
Sb	1.20	3.34	2.48	5.16	5.41	3.71	4.35	3.76	1.94	2.91	1.95	2.71
Se	0.05	0.08	0.12	0.02	0.08	0.04	0.03	0.03	0.10	0.05	0.04	0.08
S	16.50	16.39	16.27	17.01	17.34	16.26	16.59	16.06	16.69	16.20	16.52	17.20
Total	99.94	98.67	99.18	100.62	101.41	99.42	98.76	99.47	100.28	98.99	99.16	99.11
Cu	0.01	0.02	0.01	0.00	0.01	0.03	0.02	0.09	0.00	0.03	0.00	0.01
Ag	5.56	5.18	3.79	5.82	5.77	2.98	4.60	5.39	5.51	3.27	5.82	6.32
Fe	0.02	0.02	0.02	0.00	0.06	0.01	0.00	0.05	0.18	0.00	0.14	0.02
Pb	9.05	9.60	11.97	8.71	8.05	13.61	10.86	9.42	8.80	12.83	8.18	7.30
Cd	0.07	0.05	0.04	0.08	0.04	0.04	0.07	0.05	0.11	0.16	0.10	0.00
Bi	12.61	11.38	10.55	10.90	11.31	9.11	9.99	11.69	12.33	9.92	12.76	12.41
Sb	0.61	1.71	1.29	2.55	2.64	1.94	2.22	1.93	0.98	1.53	0.99	1.34
Se	0.04	0.07	0.10	0.02	0.06	0.03	0.02	0.02	0.08	0.04	0.03	0.06
S	32.04	31.97	32.23	31.93	32.07	32.25	32.22	31.37	32.02	32.29	32.00	32.49
N_{chem}	6.30	6.09	5.88	6.36	5.83	5.89	6.31	6.02	6.16	5.79	6.06	6.39
L%	67.74	64.55	48.69	70.06	73.98	38.42	56.42	66.80	68.03	42.31	72.36	77.78
x	1.46	1.32	0.95	1.53	1.42	0.75	1.22	1.34	1.41	0.80	1.47	1.71
Bi/(Bi + Sb)	0.95	0.87	0.89	0.81	0.81	0.82	0.82	0.86	0.93	0.87	0.93	0.90

empirical formula coefficients based on 60 *apfu*

n – number of point analyses; *x* – substitution coefficient of the Ag + Bi ↔ 2 Pb substitution

Tab. 10 Chemical analyses of eskimoite

Sample	ST 61gr1	ST 80fr3	ST 126A2	ST 22D	ST 116D	ST 116C	ST 186A	ST 118B
n	4	6	1	5	13	4	3	3
Phase	Esk_{69}	Esk_{72}	Esk_{66}	Esk_{75}	Esk_{71}	Esk_{66}	Esk_{73}	Esk_{76}
Cu	0.00	0.00	0.04	0.04	0.01	0.02	0.02	0.65
Ag	10.78	11.92	10.07	11.78	11.31	10.24	11.75	10.83
Fe	0.05	0.00	0.10	0.02	0.00	0.00	0.00	0.10
Pb	30.36	29.12	31.11	26.13	29.68	31.85	28.67	26.20
Cd	0.10	0.12	0.13	0.00	0.03	0.04	0.02	0.07
Bi	37.93	38.45	40.07	41.50	39.38	39.60	40.37	44.27
Sb	4.35	5.02	2.02	2.23	3.44	2.54	3.44	1.88
Se	0.08	0.05	0.00	0.05	0.00	0.00	0.00	0.00
S	16.99	16.99	16.24	17.25	16.98	17.07	17.13	17.27
Total	100.64	101.68	99.79	99.04	100.88	101.21	101.41	101.49
Cu	0.00	0.00	0.05	0.03	0.01	0.02	0.02	0.68
Ag	6.82	7.45	6.60	7.49	7.16	6.54	7.38	6.77
Fe	0.06	0.00	0.12	0.02	0.00	0.00	0.00	0.12
Pb	10.00	9.48	10.61	8.58	9.79	10.59	9.37	8.53
Cd	0.06	0.07	0.08	0.00	0.02	0.02	0.01	0.04
Bi	12.39	12.41	13.55	13.65	12.87	13.05	13.08	14.28
Sb	2.43	2.78	1.18	1.20	1.93	1.44	1.91	1.04
Se	0.07	0.04	0.00	0.03	0.00	0.00	0.00	0.00
S	36.17	35.75	35.82	36.97	36.18	36.31	36.19	36.32
N_{chem}	6.95	7.33	6.97	7.46	7.35	6.89	7.37	7.00
L%	69.04	72.40	66.21	75.22	70.51	66.23	72.61	75.82
x	1.71	1.93	1.64	2.06	1.88	1.62	1.95	1.89
Bi/(Bi + Sb)	0.84	0.82	0.92	0.92	0.87	0.90	0.87	0.93

empirical formula coefficients based on 68 *apfu*
n – number of point analyses
x – substitution coefficient of the Ag + Bi ↔ 2 Pb substitution

lianite homologues with N > 4, the Sb ↔ Bi substitution is only limited (Bi/(Bi + Sb) = 0.80–0.95, corresponding to 5.96 and 1.20 Sb *apfu*). Of other measured minor elements (Cu, Fe, Cd, Se, Te), only Cd shows increased contents (max. 0.28 wt. %).

Treasurite was detected in the powder pattern of two samples, unit-cell parameters were calculated for the space group *C2/m* suggested by Makovicky and Karup-Møller (1977b). Yet, the quality of the powder patterns is poor due to intimate intergrowths of several phases with overlapping peaks.

Eskimoite ($^{5,9}L$, N_{chem} = 7) is even rarer than treasurite; it is the first occurrence reported from the Czech Republic. Eskimoite forms grains or lamellae in quartz gangue intergrowing with other lillianite homologues and galena (Fig. 7d), on average 100 μm across. In the sample ST 80fr3 it is associated with galena, Gus_{95}, $And_{67–92}$ (Bi-rich fizelyite, ramdohrite, quatrandorite) and heyrovskýite (Hey_{34}), in ST 61 it is associated with Tr_{74}, Gus_{93}, And_{84} and galena.

Samples identified as members of the eskimoite solid solution display average N = 7.16 (range of averages is 6.95–7.33, total range 6.82–7.63). Chemical compositions and empirical formulae calculated to 68 *apfu* are listed in Tab. 10 and plotted in Figs 2 and 6. Antimony content does not exceed 5 wt. %, corresponding to 2.78 *apfu* (Z = 1); Bi/(Bi + Sb) = 0.82–0.93. The Ag^{+} + Bi^{3+} ↔ 2 Pb^{2+} substitution is in a much narrower interval between 66.2 % ($Esk_{66.2}$): $Ag_{6.65}Pb_{10.78}(Bi_{13.55}Sb_{1.18})_{\Sigma=14.69}S_{35.82}$ and 75.2 % ($Esk_{75.8}$): $Ag_{7.49}Pb_{8.58}(Bi_{13.65}Sb_{1.20})_{\Sigma=14.85}S_{36.97}$. Eskimoite compositions can be expressed as $^{6.82–7.63}Esk_{66–75}^{82–93}$.

Presence of eskimoite (monoclinic) which could be mistaken with Ag,Bi-heyrovskýite (orthorhombic) based solely on the chemical composition was confirmed by the P-XRD in one of the two samples (Tab. 11).

Tab. 11 Refined unit-cell parameters of eskimoite from Kutná Hora for the space group *Cm*

Sample	*a* [Å]	*b* [Å]	*c* [Å]	*β* [°]	*V* [Å^3]	N_{chem}	L%	Bi/(Bi + Sb)
ST 80	13.470(15)	4.097(4)	30.18(3)	93.35(2)	1662.6(5)	7.33	72.40	0.82
Ivigtut	13.459(5)	4.100(5)	30.194(8)	93.35(5)	1663.3(2)	6.21	67.90	1.00

Ivigtut – parameters of eskimoite from Ivigtut, Greenland (Makovicky and Karup-Møller 1977b)

Tab. 12 Chemical analyses of Ag–Bi heyrovskýite, erzwiesite, nakaséite and $^{5.5}$And phase (an Sb-analogue of vikingite?)

Sample	ST 80fr3	ST 126A2	ST 116D	ST 116D	ST 22B	ST 22D	ST 187B	ST 187B	ST 187B	ST 187B	ST 313	ST 22E
n	1	1	3	7	4	7	2	4	2	6	3	4
Phase	Hey_{34}	Hey_{43}	Erz_{69}	Erz_{69}	Erz_{69}	Erz_{72}	Nak_{97}	Nak_{101}	Nak_{98}	Nak_{97}	$^{5.3}$And	$^{5.2}$And
Cu	0.00	0.00	0.02	0.02	0.04	0.04	0.48	0.59	0.99	1.20	0.38	0.22
Ag	5.35	6.46	11.90	11.50	11.39	11.67	11.66	11.00	9.64	10.93	6.79	10.37
Fe	0.03	0.06	0.00	0.00	0.00	0.04	0.23	0.08	0.14	0.12	0.08	0.14
Pb	50.43	44.50	30.76	30.35	29.85	27.85	20.56	20.05	21.12	19.99	41.24	31.28
Cd	0.04	0.03	0.03	0.04	0.07	0.00	0.00	0.00	0.00	0.01	0.00	0.23
Bi	24.71	30.72	38.62	39.10	38.55	40.38	18.50	24.79	23.69	24.64	16.47	15.66
Sb	4.30	2.63	2.69	2.96	2.76	1.95	26.78	23.58	23.49	22.54	18.10	23.44
Se	0.04	0.07	0.00	0.00	0.00	0.03	0.00	0.08	0.00	0.01	0.00	0.00
S	15.86	16.32	16.79	16.93	17.30	17.20	20.39	19.90	20.64	20.29	18.53	19.59
Total	100.77	100.78	100.83	100.93	99.73	99.22	98.66	100.05	99.72	99.79	101.73	101.00
apfu	17	17	76	76	76	76	11	11	11	11	56	56
Cu	0.00	0.00	0.02	0.02	0.05	0.05	0.07	0.09	0.15	0.18	0.31	0.17
Ag	0.89	1.07	8.46	8.15	8.11	8.30	1.02	0.98	0.85	0.96	3.28	4.74
Fe	0.01	0.02	0.00	0.00	0.00	0.05	0.04	0.01	0.02	0.02	0.07	0.12
Pb	4.39	3.83	11.39	11.20	11.70	10.31	0.94	0.93	0.97	0.92	10.36	7.45
Cd	0.01	0.01	0.02	0.03	0.05	0.00	0.00	0.00	0.00	0.00	0.00	0.10
Bi	2.13	2.62	14.18	14.31	14.17	14.82	0.84	1.14	1.08	1.12	4.10	3.70
Sb	0.64	0.38	1.70	1.86	1.74	1.23	2.08	1.86	1.83	1.76	7.74	9.50
Se	0.01	0.02	0.00	0.00	0.00	0.03	0.00	0.01	0.00	0.00	0.00	0.00
S	8.92	9.07	40.19	40.39	40.79	41.15	6.01	5.97	6.11	6.02	30.10	30.15
N_{chem}	7.61	7.18	8.68	7.91	8.08	8.06	4.48	4.19	4.12	4.72	5.28	5.23
L%	34.05	42.54	68.75	69.31	69.26	71.79	96.72	101.04	98.20	97.08	53.22	73.59
x	0.95	1.10	2.30	2.50	2.10	2.17	1.20	1.11	1.04	1.32	0.87	1.21
Bi/(Bi + Sb)	0.77	0.87	0.89	0.89	0.89	0.92	0.29	0.38	0.37	0.39	0.35	0.28

Hey – heyrovkýite, Erz – erzwiesite, Nak – Bi-rich Cu-bearing andorite VI (nakaséite), $^{5.2}$And – an andorite phase with N_{chem} = 5.23 (a possible Sb-analogue of vikingite?) – sample ST 22E
n – number of point analyses
x – substitution coefficient of the Ag + Bi ↔ 2 Pb substitution

Silver–bismuth-rich heyrovskýite ($^{7.7}$L, N_{chem} = 7) forms allotriomorphic grains in association with $^{6.97}Esk_{66}$, $^{6.06–6.22}Tr_{68–72}$, $^{4.08–4.11}Gus_{93–94}$ and $^{5.53}Vik_{61}$. Only two compositions were identified to correspond to heyrovskýite solid solution (Fig. 2). One sample (ST 80fr3) is $^{7.61}Hey^{77}_{34}$, with empirical formula based on 17 *apfu* (Z = 4): $Ag_{0.90}Pb_{4.41}(Bi_{2.13}Sb_{0.64})_{\Sigma=2.77}S_{8.93}$, accompanied by $^{4.04}Gus_{95}$, $^{7.33}Esk_{72}$, $^{4.01–4.49}And_{67–92}$. The second sample (ST 126) is $^{7.18}Hey^{87}_{43}$, corresponding empirical formula $Ag_{1.07}Pb_{3.86}(Bi_{2.62}Sb_{0.38})_{\Sigma=3.00}S_{9.09}$.

Both analyses (Tab. 12) are assumed to represent heyrovskýite and not eskimoite on the basis of the substitution percentage being closer to the Ag–Bi-free heyrovskýite end of the N = 7 join and to the published analyses of heyrovskýite. Also, eskimoite present in the first sample displays an invariant composition close to N = 7 and L% = 70. Heyrovskýite could be unambiguously identified only with support of crystal structure data. However, neither suitable material for single-crystal XRD data collection is available nor the powder data collected indicated this mineral.

Erzwiesite ($^{8.8}$L, N_{chem} = 8) was described by Topa et al. (2013b). The mineral composition derived from the crystal structure is $Ag_8Pb_{12}Bi_{16}S_{40}$ (Z = 1). This composition from the original locality of Erzwies, Austria, corresponds very well to that determined in three samples from Kutná Hora (Tab. 12). Both occurrences display very similar substitution percentages of *c.* 70 % (Fig. 2). The range of mean N values from 7.91 to 8.68 (total range 7.75–8.80) is in agreement with that observed at Erzwies. Similar to all other lillianite homologues with N > 4, the Sb content is limited and the ratio Bi/(Bi + Sb) never exceeds 0.89. The composition of erzwiesite from Kutná Hora can be expressed as $^{7.91–8.68}Erz^{89–92}_{69–72}$ (Figs 2, 6).

Schirmerite (Type 2) (4 < N < 7) is a disordered phase of different proportions of slabs ^{4}L and ^{7}L (Type 2) (Moëlo et al. 2008). It was arbitrarily assigned to 21 point analyses in 15 samples from Kutná Hora based on the chemical composition (Tab. 13). Although schirmerite is usually classified as a phase with N values ranging from 4 to 7, all schirmerites described in this study have N = 4.50–4.88 with a composition between that of gustavite and vikingite. Antimony content does not exceed 10 mol. %, Bi/(Bi + Sb) is between 0.79 and 0.93 – a trend observed in all lillianite homologues with N > 4. Substitution percentage L% varies from 60.6 to 88.3.

Tab. 13 Chemical analyses of schirmerite (Type 2)

Sample	ST 40Bgr1	ST 42Cgr2	ST 42Dgr1	ST 52gr1	ST 62	ST 85gr2	ST 114	ST 114	ST 126A2	ST 155A	ST 167B	ST 214A5	ST 103g1t
n	1	1	1	1	2	1	1	1	1	1	1	1	1
Phase	$^{4.8}$Sch	$^{4.8}$Sch	$^{4.9}$Sch	$^{4.7}$Sch	$^{4.6}$Sch	$^{4.6}$Sch	$^{4.5}$Sch	$^{4.7}$Sch	$^{4.6}$Sch	$^{4.5}$Sch	$^{4.8}$Sch	$^{4.9}$Sch	$^{4.8}$Sch
Cu	0.00	0.01	0.03	0.00	0.01	0.00	0.04	0.07	0.07	0.02	0.01	0.02	0.01
Ag	8.48	9.28	9.08	9.15	7.74	9.12	7.54	8.48	10.06	6.82	7.16	10.95	7.21
Fe	0.02	0.00	0.01	0.07	0.00	0.00	0.03	0.04	1.31	0.26	0.02	0.03	0.00
Pb	27.35	26.80	27.83	24.31	30.02	25.37	30.24	27.13	19.42	33.42	32.14	21.98	31.58
Cd	0.12	0.08	0.05	0.13	0.12	0.04	0.13	0.04	0.00	0.05	0.17	0.06	0.14
Bi	44.86	41.94	43.02	45.75	44.17	45.59	39.12	39.53	37.17	38.47	39.89	45.48	37.18
Sb	2.07	5.32	4.40	2.62	2.57	3.54	5.64	6.14	10.63	5.74	3.26	5.42	4.94
Se	0.06	0.06	0.05	0.07	0.26	0.10	0.01	0.05	0.09	0.03	0.10	0.08	0.10
S	17.09	17.24	17.06	16.83	17.19	17.48	17.28	16.72	19.15	17.24	16.51	18.17	16.68
Total	100.05	100.74	101.53	98.94	102.08	101.23	100.02	98.20	97.89	102.05	99.27	102.20	97.84
Cu	0.00	0.01	0.02	0.00	0.00	0.00	0.02	0.04	0.03	0.01	0.00	0.01	0.00
Ag	2.65	2.84	2.79	2.88	2.39	2.79	2.33	2.66	2.86	2.09	2.29	3.23	2.30
Fe	0.01	0.00	0.00	0.04	0.00	0.00	0.02	0.02	0.72	0.15	0.02	0.02	0.00
Pb	4.46	4.27	4.46	3.99	4.83	4.04	4.86	4.44	2.88	5.33	5.35	3.37	5.24
Cd	0.04	0.02	0.01	0.04	0.04	0.01	0.04	0.01	0.00	0.02	0.05	0.02	0.04
Bi	7.25	6.63	6.83	7.44	7.04	7.19	6.24	6.41	5.46	6.08	6.58	6.91	6.12
Sb	0.57	1.44	1.20	0.73	0.70	0.96	1.54	1.71	2.68	1.56	0.92	1.41	1.39
Se	0.03	0.03	0.02	0.03	0.11	0.04	0.01	0.02	0.03	0.01	0.04	0.03	0.04
S	17.99	17.76	17.66	17.85	17.87	17.97	17.96	17.68	18.33	17.76	17.75	18.00	17.89
N_{chem}	4.80	4.82	4.87	4.72	4.61	4.59	4.54	4.65	4.58	4.50	4.84	4.88	4.80
L%	73.43	77.16	75.09	80.19	68.64	80.26	68.11	75.41	85.55	60.59	62.02	88.29	63.22
x	1.03	1.09	1.08	1.09	0.90	1.04	0.86	1.00	1.10	0.76	0.88	1.27	0.88
Bi/(Bi + Sb)	0.93	0.82	0.85	0.91	0.91	0.88	0.80	0.79	0.67	0.80	0.88	0.83	0.81

empirical formula coefficients based on 33 *apfu*
n – number of point analyses
x – substitution coefficient of the Ag + Bi ↔ 2 Pb substitution

The variations of measured schirmerite compositions can be summarized as $^{4.42–4.88}Sch^{79–93}_{61–88}$.

4.2. *Lillianite homologues with Sb > Bi: andorite branch*

Minerals of the andorite series occur in the ore with gustavite, terrywallaceite and other Bi-sulphosalts. They form allotriomorphic grains, up to several millimetres, in quartz, intergrown or associated with other lillianite homologues and galena (Fig. 7a). Most frequently they form rims of gustavite grains, with a clear trend of rimward enrichment in Sb. It is the first occurrence of bismuthian andorite reported from the Czech Republic. Chemical compositions of 38 samples (118 point analyses) were identified as members of andorite branch, i.e. lillianite homologues with N = 4, Sb > Bi (Bi/(Bi + Sb) < 0.5: 0.49–0.23) and percentage of the $Ag^{+} + Sb^{3+} \leftrightarrow 2\ Pb^{2+}$ substitution between 64.6 % and 92.3 %. Bi-rich andorite VI (nakaséite) with a substantial Cu content has the substitution between 95.6 and 104.6 % and Bi/(Bi + Sb) = 0.29–0.42. As in the case of Bi-based lillianites, all samples exhibit two major substitutions: (1) "andorite" substitution $Ag^{+} + Sb^{3+} \leftrightarrow 2\ Pb^{2+}$ and (2) $Bi^{3+} \leftrightarrow Sb^{3+}$ substitution. The latter forms a chemically continuous series from Bi-rich andorite through staročeskeite to terrywallaceite to gustavite (Figs 3, 6) which can be observed even within one grain (Tab. 6, Electronic Supplementary Material 1). No Bi-free andorites were found in any of the studied samples in this paragenesis. In BSE images the increasing Sb content is indicated by darker

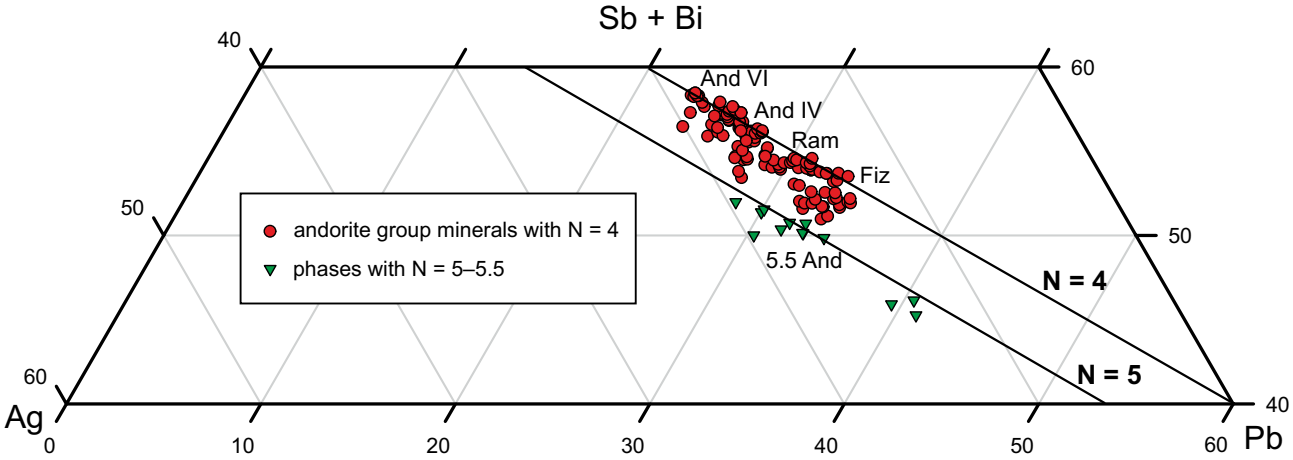

Fig. 8 Ternary diagram of the system Ag_2S–(Sb_2S_3 + Bi_2S_3)–PbS showing the andorite substitution $Ag^+ + (Sb,Bi)^{3+} \leftrightarrow 2\ Pb^{2+}$ (andorite series) in 38 samples of lillianite homologues with Sb > Bi from Kutná Hora. Two groups of compositions are present: (1) red circles – points with N = 4 (andorite) and (2) green triangles – points with N = 5.0–5.5, (a possible Sb analogue of vikingite). A number of andorite analyses fall between andorite IV and ramdohrite which is interpreted as an intergrowth of the two andorite phases.

shades of grey but often no discernible grain boundaries were observed. Concerning the relation between Sb, L% and N_{chem}, prevailing is the trend B, marked by a negative correlation between Sb content and L% and positive one between Sb and N (Fig. 5).

In the Ag–(Sb + Bi)–Pb ternary diagram (Fig. 8) a number of analyses falls between ramdohrite and andorite IV (quatrandorite). They obviously represent submicroscopic intergrowths of several andorite phases, a phenomenon that was observed from other localities as well. In this paper, analyses with L% = 85–93 were arbitrarily assumed to represent andorite IV (quatrandorite), those with L% = 70–79 Bi-rich ramdohrite, and with L% = 64–69 Bi-rich fizelyite. Andorite compositions with increased Bi content were determined by Moëlo et al. (1989). Empirical formulae of andorite phases with L% < 100 were calculated on the basis of 44 *apfu* (Z = 4), in order to make the comparison between various compositions easier (Tab. 6).

The discovery of oscarkempffite $Ag_{10}Pb_4(Sb_{17}Bi_9)S_{48}$ (Topa et al. 2011) and clinooscarkempffite, $Ag_{15}Pb_6Sb_{21}Bi_{18}S_{72}$ (Topa et al. 2013a), both with substantial Bi contents, made the situation in the Sb-rich group of the lillianite family even more complex. Both have N = 4, characterized by an oversubstitution of 124 and 125 %, respectively (Makovicky and Topa 2014). These minerals have not been found in Kutná Hora so far. However, with regard to the fact that terrywallaceite, another lillianite homologue with constituent Bi and Sb, is abundant among bismuth sulphosalts, finding of these two minerals is possible in future.

4.2.1. Antimonian lillianite homologues with N = 4

Bi-rich andorite IV (quatrandorite). Twelve samples (24 microprobe analyses) with andorite substitution L% = 85–93 were assigned to andorite IV (quatrandorite). Average N = 4.02 (total range 3.72–4.26), the andorite substitution ranges from 85.3 to 92.3 %, Bi ↔ Sb substitution shows no compositional gap, Bi/(Bi + Sb) = 0.30–0.46 (Figs 3, 6). The andorite IV compositions can be summarized as $^{3.72–4.26}And^{30–46}_{85.3–92.3}$ (Tab. 6).

Andorite IV was identified chemically and confirmed by P-XRD. However, of the total 111 measured points in andorite (Sb > Bi), 36 points display compositions corresponding to $And_{80–90}$. These do not belong to any of the four defined andorite minerals and in fact represent a submicroscopic intergrowth of And IV with ramdohrite or fizelyite, or both (Figs 3, 7a).

Of all measured andorite analyses only four samples fell into the range of "typical" quatrandorite composition $And_{90–93}$. All four have N = 4.00–4.05. The formula of the sample ST 80fr3, close to the ideal quatrandorite, is $Ag_{3.75}Pb_{4.72}(Sb_{7.28}Bi_{4.57})_{\Sigma=11.85}S_{23.67}$ ($^{4.03}And^{39}_{91.7}$). Chemical compositions and empirical formulae are calculated to 44 atoms.

Bi-rich ramdohrite. Chemical composition of 25 samples (56 point analyses) was identified as ramdohrite with average N = 4.12 (3.91–4.41) and Bi/(Bi + Sb) = 0.30–0.46 (Figs 3, 8). Ramdohrite was arbitrarily ascribed to points with compositions $And_{71–79}$ (Tab. 6, Electronic Supplementary Material 1). Ramdohrite compositions from Kutná Hora can be expressed as $^{3.91–4.41}And^{30–46}_{71–79}$. A typical example of Bi-rich ramdohrite is sample ST 25 whose formula (7 point analyses, Electronic Supplementary material 1), can be expressed as $(Ag_{2.95}Cu_{0.02})_{\Sigma=2.97}(Pb_{6.07}Fe_{0.06}Cd_{0.08})_{\Sigma=6.21}(Sb_{5.96}Bi_{4.76})_{\Sigma=10.72}(S_{24.13}Se_{0.03})_{\Sigma=24.16}$ corresponding to $^{4.12}And^{44}_{72.4}$.

No minor elements have been found in Bi-rich ramdohrite. Contents of Cu, Fe, Cd and Se are below detection limits. Bi-rich ramdohrite is the most common of

Tab. 14 Refined unit-cell parameters of Bi-rich ramdohrite from Kutná Hora for the space group $P2_1/n$ in comparison with the structure (Makovicky and Makovicky 1983)

sample	*a* [Å]	*b* [Å]	*c* [Å]	*β* [°]	*V* [Å³]
ST 80	19.239(2)	13.080(11)	8.732(8)	90.34(1)	2197.3
structure	19.24	13.08	8.73	90.28	2197

all andorite compositions and was also confirmed by P-XRD in six samples (Tab. 14). Unlike most other lillianite homologues, it can be well distinguished by the presence of two sets of reflections d_{-212}, d_{212} and d_{-312}, d_{312} which do not coincide with other reflections that are often present in the bulk sample. Unit-cell parameters of the measured sample from Kutná Hora are almost identical to Bi-free ramdohrite from the structure (Tab. 14), which can be explained by the presence of two substitutions in our sample. While higher substitution percentage (L%) decreases the volume (and the *a* parameter), the $Bi^{3+} \leftrightarrow Sb^{3+}$ substitution increases it. Again, like in the case of gustavite, the unit-cell parameters refined for samples displaying multiple substitutions do not provide the information usually expected from this calculation.

Bi-rich fizelyite. Six samples (13 point analyses) with mean andorite substitution percentage of 67.9 (64.6–69.5) were arbitrarily assigned to fizelyite, ideal composition $Pb_7Ag_{2.5}Sb_{10.5}S_{24}$ (Z = 4). No analytical points with a lower degree of the $Ag^+ + Sb^{3+} \leftrightarrow 2\ Pb^2$ substitution were found (Tab. 6, Electronic Supplementary Material 1). The parameter N_{chem} varies between 3.94 and 4.29 (mean 4.07), Bi/(Bi + Sb) between 0.24 and 0.38. The closest to ideal fizelyite (represented by points with the lowest L% and Bi/(Bi + Sb)) is the sample ST 89 with N = 4.21, L%= 65.7, Bi/(Bi + Sb) = 0.24 and the empirical formula $(Ag_{2.81}Cu_{0.02})_{\Sigma=2.83}(Pb_{6.77}Fe_{0.06}Cd_{0.04})_{\Sigma=6.87}(Sb_{8.06}Bi_{2.60})_{\Sigma=10.66}(S_{23.61}Se_{0.03})_{\Sigma=23.64}$.

Microprobe points with compositions $And_{64–69}$ were less common than $And_{70–79}$. Similar to ramdohrite, unambiguous determination of particular andorite phase present in the sample would be possible only on the basis of single-crystal XRD analysis.

Three samples (9 point analyses) exhibit average N = 4.51 (4.38–4.67), L%= 69.28 (66.7–72.1). The range of Bi/(Bi + Sb) (0.25–0.32) is narrower than in ramdohrite and andorite IV; no transition to a phase with Bi : Sb = 1 : 1 takes place. Chemical compositions and formulae calculated to 13 *apfu* are in Electronic Supplementary Material 1. Of all measured minor elements, Cd is elevated in one sample (max. 0.23 wt. %). The composition of this phase with N ~ 4.5 ($^{4.5}And_{69}$) corresponds well to the Ag-excess fizelyite. The structure of this mineral was determined by Yang et al. (2009) and the composition that they have reported corresponds to N = 4.4 and L% = 65.5.

Bi-rich Cu-bearing andorite VI (Bi-rich nakaséite). Nakaséite was defined by Ito and Muraoka (1960) as a Cu-rich derivative of andorite with a superstructure of ($c \times 24$). A later detailed examination of the andorite–fizelyite series minerals (Moëlo et al. 1989) confirmed that nakaséite is an oversubstituted, Cu-rich (~ 1 wt. %) variety of andorite VI, with a formula close to $(Ag_{0.93}Cu_{0.13})_{\Sigma=1.06}Pb_{0.88}Sb_{3.06}S_6$.

Nakaséite was found in Kutná Hora in five different grains of one sample (20 point analyses), The $Ag^+ + Sb^{3+} \leftrightarrow 2\ Pb^2$ substitution is between 95.6 and 104.6 %, Cu varies between 0.37 and 2.00 wt. % and Bi/(Bi + Sb) ranges from 0.29 to 0.42 (Tab. 12). Nakaséite in the sample ST 187B is associated with Bi-rich berthierite, Bi-rich boulangerite, terrywallaceite, a mineral close to Sb-rich bismuthinite but containing Ag and Cu up to 1 wt. % and a phase resembling berryite ($Cu_3Ag_2Pb_3Bi_7S_{16}$) but having one third of Bi atoms replaced by Sb. Because natural bismuthinite does not accommodate Ag and Cu and berryite does not incorporate such high amounts of Sb, the crystal structure of both phases will be further investigated.

4.2.2. Minerals with N = 5.0–5.5

$^{5}And_{68}$ phase. One sample with a composition $^{5}And_{68}$ phase (6 point analyses) shows average N_{chem} = 5.01 (4.87–5.19) and a very similar substitution percentage as the $^{4.5}And_{69}$ phase described above. Average L% is 68.1 (65.09–70.07). The Bi ↔ Sb substitution is limited, Bi/(Bi + Sb) = 0.23–0.24. The phase is associated with Bi-rich boulangerite and Ag,Bi-bearing galena. A general charge-balanced formula obtained from the ratio of atomic percentages could be $Ag_8Pb_{15}Sb_{23}S_{54}$ or $Ag_{16}Pb_{30}Sb_{46}S_{107}$. Expressed in the same ratios as the $^{4.5}And_{69}$ phase, the formula calculated to 13 *apfu* is $Ag_{1.03}Pb_{1.94}(Sb_{2.33}Bi_{0.70})_{\Sigma=3.03})S_{7.00}$. Chemical compositions and formulae calculated to 13 atoms are in Electronic Supplementary Material 1 and point analyses are plotted in Figs 3 and 8. Copper and cadmium contents are elevated, the former coupled with Ag, the latter with Pb. This phase may structurally belong to the Ag-excess fizelyite of Yang et al. (2009).

$^{5.5}And$ phase (a possible Sb-analogue of vikingite). Two samples (7 point analyses) with compositions having N > 5 and Sb > Bi were detected (Tab. 12). Formula coefficients were calculated to 56 *apfu* in order to match the formula of vikingite (Z = 1). The two samples differ mutually in the substitution percentage and Sb content (albeit in both cases Sb > Bi). On the other hand, they share common features: very similar N values and the presence of Cu, normally unknown in bismuthian lillianite homologues from Kutná Hora. The first sample (ST 313A) displays an average N = 5.28 (5.09–5.39), Bi/(Bi + Sb) = 0.35 and the Ag + (Bi,Sb) ↔ Pb substitution is 53.22 %, expressed by the formula $Ag_{3.28}Pb_{10.36}(Bi_{4.10}Sb_{7.74})_{\Sigma=11.84}S_{30.10}$. This sample may

be either an undersubstituted lillianite homologue or it may represent an extremely Bi-rich owyheeite. The second sample (ST 22E) has an average N = 5.23 (5.05–5.63), Bi/(Bi + Sb) = 0.28 and the Ag + (Sb,Bi) ↔ 2Pb substitution is 73.59 %, leading to the formula $Ag_{4.74}Pb_{7.45}(Bi_{3.70}Sb_{9.50})_{\Sigma=13.20}S_{30.15}$ and this phase may represent a potential Sb-analogue of vikingite. The single-crystal XRD analysis is necessary to determine the structure of the phase and to assess its relationship to other minerals of the series. An interesting feature of both compositions are increased contents of Cu (max. 0.51 wt. %) in both samples and of Cd (max. 0.32 wt. %) in the second sample. At the same time, both elements are absent in the surrounding phases, gustavite and Bi-rich andorite IV (Tab. 12).

5. Conclusions

Bismuth sulphosalt minerals belonging to the lillianite homologous series are described from the Kutná Hora ore district (60 km east of Prague). The following Bi members were identified: gustavite, terrywallaceite, staročeskéite (IMA No. 2016-101), vikingite, treasurite, eskimoite, (Ag, Bi)-rich heyrovskýite, erzwiesite and schirmerite (Type 2). The Sb-based members include: Bi-rich andorite IV (quatrandorite), Bi-rich ramdohrite, Bi-rich fizelyite, Bi-rich Cu-bearing andorite VI (nakaséite) and a mineral phase with N = 5.0–5.5, a possible Sb-analogue of vikingite. Relations between Ag + Bi ↔ 2 Pb and Sb ↔ Bi substitutions were found, trends within multicompositional grains observed. New substitution limits have been observed in lillianite homologues, as follows.

For the lillianite homologues with N = 4:

(1) Chemical analyses show a complete solid solution along the lillianite ($Pb_3Bi_2S_6$) – gustavite ($AgPbBi_3S_6$) join from 60 to 113 % of $Ag^+ + Bi^{3+} \leftrightarrow 2\ Pb^{2+}$ substitution with no miscibility gap. However, the results of the crystal structure studies do not support the complete solid solution and consequently the samples with 60–75 % substitution probably represent mixtures of two exsolved components: gustavite and lillianite.

(2) A complete solid solution along $AgPbBi_3S_6$–$AgPbSb_3S_6$ join from Bi/(Bi + Sb) = 0.97 to Bi/(Bi + Sb) = 0.23 corresponds to 3–78 at.% of Bi substituted by Sb with no miscibility gap. In the Bi-lillianite branch, the ratio Bi/(Bi + Sb) ranges from 0.50 to 0.97 and in the andorite branch this ratio varies between 0.49 and 0.23.

(3) Oversubstituted gustavite compositions with L% >100 are Sb-rich. All samples with Bi/(Bi + Sb) = 0.50–0.75 correspond to terrywallaceite, only a few have Bi/(Bi + Sb) > 0.75 and are gustavite.

(4) Undersubstituted gustavite with L% between 60 and 85 is usually Sb poor.

(5) Transitional members with Bi/(Bi + Sb) ~ 0.47–0.53 and L% = 66–78 belong to the recently approved mineral staročeskéite (IMA No. 2016-101).

(6) Bi-rich andorites have L% = 66–92 %; Bi-rich nakaséite with a substantial Cu content has the substitution percentages between 95.6 and 104.6 %.

(7) None of the analysed samples contain gustavite without at least some antimony. The lowest detected content of Sb in gustavite is 0.98 wt. % (Bi/(Bi + Sb) = 0.97).

For the lillianite homologues with N > 4:

(1) The substitution of Bi by Sb is limited, solid-solution field is narrow compared to minerals with N = 4, from 5 to 25 at. % Bi being substituted by Sb. The Bi/(Bi + Sb) ratios vary; the range attains 0.75–0.95 for vikingite and 0.81–0.95 for treasurite. For homologues with higher N_{chem} values it is even more limited: 0.82–0.93 for eskimoite and 0.89–0.92 for erzwiesite.

(2) The extent of Ag + Bi ↔ Pb substitution is more limited than for lillianite minerals with N = 4. Vikingite and treasurite show a fairly wide extent of Ag + Bi ↔ Pb substitution 47–70 %, and 38–74 %, respectively. Higher homologues with N > 6 display much narrower ranges, 66–76 % for eskimoite and only 69–72 % for erzwiesite.

A complete series from gustavite with no Sb, through terrywallaceite and transitional members with Bi/(Bi + Sb) = 0.50 represented by staročeskéite, to andorite with Bi/(Bi + Sb) = 0.23 was found in the Kutná Hora ore district. These chemical variations can be observed even within a single grain.

Two main trends relating the percentage of the Ag + Bi ↔ 2 Pb substitution (L%), Bi ↔ Sb substitution (i.e. the Bi/(Bi + Sb) ratio) and N_{chem} were observed:

(1) increase in Sb and L% accompanied by decrease of N (trend A), and

(2) increase in Sb and N accompanied by decrease in L% (trend B).

Trend A is the most frequently encountered and is typical of gustavite and terrywallaceite compositions (Bi > Sb). There is a positive correlation between Sb content and the L% (i.e. oversubstituted gustavite is Sb-richer than undersubstituted gustavite) accompanied by the decrease of N. The exactly opposite trend B is typical of andorite compositions (Sb > Bi): Sb is negatively correlated with L% (fizelyite is poorer in Bi than quatrandorite), and positively with N. The range of the $Bi^{3+} \leftrightarrow Sb^{3+}$substitution in lillianite homologues with N = 4 found in the Kutná Hora samples has not been observed before and is exceptional worldwide.

In general, the minerals of veins of the Kutná Hora ore district followed a succession from Sb-poor to Sb-rich minerals: native Bi – galena – eskimoite/erzwiesite/treasurite/vikingite – gustavite – terrywallaceite –

staročeskéite – Bi-rich andorite minerals – Bi-rich Pb–Sb sulphosalts (jamesonite, boulangerite).

The study also revealed that the silver-rich character of the pyrite ores of the Startočeské pásmo Lode eagerly mined in the Middle Ages is caused not only by microscopic inclusions in base sulphides, but also macroscopic aggregates of Ag–Pb–Bi–Sb sulphosalts (mostly lillianite homologues) and Ag–Bi galena.

Acknowledgements. I would like to sincerely thank to Dan Topa (Naturhistorisches Museum, Wien) for all his guidance and being my tutor, Jiří Sejkora (National Museum, Prague) for a valuable help with the manuscript preparation and electron microprobe analyses, Emil Makovicky (Geological Institute, University of Copenhagen) for consultations on lillianite homologues, Vladimír Šrein (Czech Geological Survey, Prague) for consultations about geological and geochemical aspects of the Kutná Hora deposit, Jaroslav Maixner (University of Chemistry and Technology Prague) for help with powder data collection and procession, and to Zuzana Cílová (University of Chemistry and Technology, Prague) for EDS analyses. Thanks go to Roman Skála for editorial help and to an anonymous reviewer for general hints on changing the manuscript. Editor-in-chief Vojtěch Janoušek is acknowledged for comments and suggestions that greatly helped to improve the manuscript. This research was financially supported by the project 15-18917 S of the Czech Science Foundation**.**

Electronic supplementary material. The chemical analyses of lillianite homologues with N = 4 are available online at the Journal web site (*http://dx.doi.org/10.3190/jgeosci.235*).

References

Cook NJ (1997) Bismuth and bismuth–antimony sulphosalts from Neogene vein mineralization, Baia Borsa area, Maramures, Romania. Mineral Mag 61: 387–409

Degen T, Sadki M, Bron E, König U, Nénert G (2014) The HighScore suite. Powder Diffr 29: S13–S18

Fergusson IF, Rogerson AH, Wolstenholme JFR, Hughes TE, Huyton A (1987) Firestar-2. A computer program for the evaluation of X-ray powder measurements and the derivation of crystal lattice parameters. Risley Nuclear Power Development Establishment, Warrington, UK

Harris DC, Chen TT (1975) Gustavite: two Canadian occurrences. Canad Mineral 13: 411–414

Holub M (2009) Estimate of the amount of silver contained in ore mined from Staročeské pásmo Lode. Kutnohorsko vlastivěd sbor 11: 30–44 (in Czech)

Holub M, Hoffman V, Mikuš M. Trdlička Z (1982) Polymetallic mineralization of the Kutná Hora ore district. Sbor Geol věd, Ložisk Geol Mineral 23: 69–123 (in Czech)

Ito T, Muraoka H (1960) Nakaséite, an andorite-like new mineral. Z Kristallogr 113: 94–98

Makovicky E, Karup-Møller S (1977a) Chemistry and crystallography of the lillianite homologous series, part I. General properties and definitions. Neu Jb Mineral, Abh 130: 265–287

Makovicky E, Karup-Møller S (1977b) Chemistry and crystallography of the lillianite homologous series, part II. Definition of new minerals: eskimoite, vikingite, ourayite and treasurite. Redefinition of schirmerite and new data on the lillianite–gustavite solid solution series. Neu Jb Mineral, Abh 131: 56–82

Makovicky E, Makovicky M (1983) The crystal structure of ramdohrite, $Pb_6Sb_{11}Ag_3S_{24}$, and its implications for the andorite group and zinckenite. Neu Jb Mineral, Abh 147: 58–79

Makovicky E, Topa D (2014) Lillianites and andorites: new life for the oldest homologous series of sulfosalts. Mineral Mag 78: 387–414

Makovicky E, Mumme WG, Madsen IC (1992) The crystal structure of vikingite. Neu Jb Mineral, Mh 10:454–468

Malec J, Pauliš P (1997) Kutná Hora ore mining district and appearances of past mining and metallurgic activities on its territory. Bull mineral-petrolog Odd Nár Muz (Praha) 4–5: 86–105 (in Czech)

Moëlo Y, Makovicky E, Karup-Møller S (1989) Sulfures complexes plombo-argentifères: minéralogie et cristallochimie de la série andorite–fizélyite, $(Pb,Mn, Fe,Cd, Sn)_{3-2x}(Ag, Cu)_x(Sb, Bi,As)_{2+x}(S, Se)_6$. Documents du BRGM 167: pp 1–107

Moëlo Y, Makovicky E, Mozgova NN, Jambor JL, Cook N, Pring A, Paar W, Nickel EH, Graeser S, Karup-Møller S, Balic-Zunic T, Mumme WG, Vurro F, Topa D, Bindi L, Bente K, Shimizu M (2008) Sulfosalt systematics: a review. Report of the sulfosalt sub-committee of the IMA Commission on Ore Mineralogy. Eur J Mineral 20: 7–46

Otto HH, Strunz H (1968) Zur Kristallchemie synthetischer Blei–Wismut–Spießglanze. Neu Jb Mineral, Abh, 108: 1–19

Oxford Diffraction (2008) CrysAlis *RED*, CCD data reduction GUI. Rigaku Oxford Diffraction Ltd., Oxford, UK

Palatinus L, Chapuis G (2007) Superflip – a computer program for the solution of crystal structures by charge flipping in arbitrary dimensions. J Appl Cryst 40: 786–790

Pauliš P (1998) Minerals of Kutná Hora ore district. Kuttna, Kutná Hora, pp 1–48 (in Czech)

Pažout R, Dušek M (2009) Natural monoclinic $AgPb(Bi_2Sb)_3S_6$, Sb-rich gustavite. Acta Crystallogr, Sect C Cryst Struct 65: i77–i80

Pažout R, Dušek M (2010) Crystal structure of natural orthorhombic $AgPbBi_{1.75}Sb_{1.25}S_6$, a lillianite homologue

with N = 4; comparison with gustavite. Eur J Mineral 22: 741–750

Pažout R, Ondruš P, Šrein V (2001) Gustavite with variable Bi/Sb ratio from Kutná Hora deposit, Czech Republic, a new occurrence. Neu Jb Mineral, Mh 4: 157–168

Pažout R, Sejkora J, Šrein V (2017) Bismuth and bismuth–antimony sulphosalts from Kutná Hora vein Ag–Pb–Zn ore district, Czech Republic. J Geosci 62: 59–76

Petříček V, Dušek M, Palatinus L (2006) Jana2006. Structure Determination Software Programs. Institute of Physics, Prague, Czech Republic

PDF-2, McClune F (ed) (2005) Powder Diffraction File. International Centre for Diffraction Data (ICDD), 12 Campus Boulevard, Newton Square, Pennsylvania, 19073–3272

Pouchou JL, Pichoir F (1985) "PAP" (φρZ) procedure for improved quantitative microanalysis. In: Armstrong JT (ed) Microbeam Analysis. San Francisco Press, San Francisco, pp 104–106

Stoe & Cie (1998) X-SHAPE. Sto & Cie, Darmstadt, Germany

Topa D, Makovicky E (2011) The crystal structure of gustavite, $PbAgBi_3S_6$. Analysis of twinning and polytypism using the OD approach. Eur J Mineral 23: 537–550

Topa D, Makovicky E, Paar WH, Stanley CJ, Roberts AC (2011) Oscarkempffite, IMA 2011–029. CNMNC Newsletter No. 10. Mineral Mag 75: 2601–2613

Topa D, Makovicky E, Paar WH (2013a) Clino-oscarkempffite, IMA 2012-086. CNMNC Newsletter No. 16. Mineral Mag 77: 2695–2709

Topa D, Makovicky E, Zagler G, Putz H, Paar WH (2013b) Erzwiesite, IMA 2012-082. CNMNC Newsletter No. 15. Mineral Mag 77: 1–12

Yang H, Downs RT, Burt JB, Costin G (2009) Structure refinement of an untwinned single crystal of Ag-excess fizélyite, $Ag_{5.94}Pb_{13.74}Sb_{20.84}S_{48}$. Canad Mineral 47: 1257–1264

Yang H, Downs RT, Evans SH, Pinch WW (2013) Terrywallaceite, $AgPb(Sb,Bi)_3S_6$, isotypic with gustavite, a new mineral from Mina Herminia, Julcani Mining District, Huancavelica, Peru. Amer Miner 98: 1310–1314